Effects of Air Quality on Housing Location: A Predictive Dynamic Continuum User-Optimal Approach

Liangze Yang¹, S.C. Wong², H.W. Ho³, Mengping Zhang⁴ and Chi-Wang Shu⁵

Abstract

Recent decades have seen increasing concerns regarding air quality in housing locations. This study proposes a predictive continuum dynamic user-optimal model with combined choice of housing location, destination, route, and departure time. A traveler's choice of housing location is modeled by a logit-type demand distribution function based on air quality, housing rent, and perceived travel costs. Air quality, or air pollutants, within the modeling region are governed by the vehicle-emission model and the advection-diffusion equation for dispersion. In this study, the housing-location problem is formulated as a fixed-point problem, and the predictive continuum dynamic user-optimal model with departure-time consideration is formulated as a variational inequality problem. The Lax-Friedrichs scheme, the fast-sweeping method, the Goldstein-Levitin-Polyak projection algorithm, and self-adaptive successive averages are adopted to discretize and solve these problems. A numerical example is given to demonstrate the characteristics of the proposed housing-location choice problem with consideration of air quality and to demonstrate the effectiveness of the solution algorithms.

Key Words: predictive dynamic user-optimal model; departure time; variational inequality; continuum model; housing location choice.

¹School of Mathematical Sciences, University of Science and Technology of China, Hefei, Anhui 230026, P.R. China. E-mail: lzeyang@mail.ustc.edu.cn.

²Department of Civil Engineering, The University of Hong Kong, Pokfulam Road, Hong Kong, PR China. E-mail:hhecwsc@hku.hk.

³Department of Civil and Environmental Engineering, The Hong Kong Polytechnic University, Hung Hom, Hong Kong, PR China. E-mail: hwai.ho@gmail.com.

⁴School of Mathematical Sciences, University of Science and Technology of China, Hefei, Anhui 230026, P.R. China. E-mail: mpzhang@ustc.edu.cn.

⁵Division of Applied Mathematics, Brown University, Providence, RI 02912, USA. E-mail: chi-wang_shu@brown.edu.

1 Introduction

The choice of a housing, or residential, location for individuals and households is fundamental in determining the demand locations that are crucial for the development of various types of transport (e.g., road pricing, transit design) and land-use planning (e.g., allocation of housing developments, locating community facilities) models. Owing to its importance and usefulness, the choice of housing location has long been a primary concern of researchers, planners, and decision makers (Schirmer et al., 2014).

In the literature, studies of housing location have widely been modeled via the trade-off between housing rent and transportation cost (Wheaton, 1977; Diamond, 1980; Giuliano, 1989). Wheaton (1977) adopted a utility-maximization approach that was also considered by Alonso (1964) and by Muth (1969) to determine housing locations in a monocentric city in which all places of employment were at the sole city center. Wheaton (1977) showed analytically that housing location is dependent upon the elasticities of land/housing demand and marginal travel cost with respect to individual or household income. Although these studies (Alonso, 1964; Muth, 1969; Wheaton, 1977; Diamond, 1980) could provide an analytical solution for the optimal housing location, most criticisms fall on their assumption of a monocentric model in which all places of employment and destinations of travel trips are located in the sole city center (Giuliano, 1989).

To resolve this problem, Owawa and Fujita (1980) and Gordon et al. (1986) developed housing-location models for polycentric cities with support from empirical examples. One of the key inputs in these housing-location models is the housing rent/cost at various locations. The hedonic prices theory (Rosen, 1974), which explains the price equilibrium between the buyer and producer, has been widely used to study housing rent. Orford (2000) proposed a multilevel modeling approach to handle the discrepancy between the theoretical and empirical application of the hedonic housing pricing model, whereas Hawkins and Habib (2018) proposed a spatiotemporal hedonic housing-price model for empirical application in Toronto. However, Ellickson (1981) suggested that the estimated hedonic price function, and thus the

aforementioned housing-location models (Wheaton, 1977; Diamond, 1980; Giuliano, 1989), could not fully and comprehensively represent the housing location choice behavior of consumers, which is substantially influenced by various factors (e.g., housing market, transportation, community facilities). To more flexibly and comprehensively model the factors that affect consumers' choice of housing location, the focus has recently been put on the use of discrete choice models, especially various types of logit-based choice models, to model the housing location choice (Ben-Akiva and Bowman, 1998; Bhat and Guo, 2004; Sener et al., 2011; Haque et al., 2019). In these studies, a large variety of factors—such as housing rent, unit size, housing type, household characteristics, built environment, amount of open space, community facilities, transportation facilities, and accessibility (Schirmer et al., 2014) — have been considered in the utility function for the housing location choice, and the trade-offs between these factors have been specifically modeled. These discrete-choice—based housing location choice models have also been successfully implemented in various empirical studies (Pinjari et al., 2011; Zolfaghari et al., 2012).

In housing location models, the transportation cost has always been the key aspect that consumers/travelers must consider/trade-off with other aspects (e.g., housing rent) in making their housing-location choice. In the aforementioned housing-location models, which are mainly choice models, the transportation time/cost is typically exogenously defined (Sener et al., 2011; Pinjari et al., 2011). To model the transportation cost in greater detail (e.g., to explicitly consider the travel time/cost of each link, or the route choice behavior of travelers), various types of traffic equilibrium model have been used to evaluate the component of transportation cost (Boyce and Mattsson, 1999; Yim et al., 2011; Li et al., 2017). Some of these housing-location models have been formulated as bilevel models (Chang and Mackett, 2006) in which housing location and traffic equilibrium are formulated as the upper- and lower-level models, respectively. However, most studies have adopted an integrated approach in which the transportation and housing equilibrium are formulated in a single lower-level model, with the upper-level model focused on various design aspects such as allocation of housing units

(Boyce and Mattsson, 1999) and optimal toll design (Li et al., 2017).

To realistically model travel cost and choice, traffic equilibrium models adopted for housing location studies are advanced from the standard user equilibrium model (Boyce and Mattsson, 1999) to user equilibrium model with stochastic route and/or housing location choice (Li et al., 2014; Ying, 2015; Ng and Lo, 2015; Li et al., 2017) and user equilibrium model with stochastic supply (link capacity) and demand (Yim et al., 2011). The above traffic equilibrium models are discrete modeling approaches, in which the transportation network is modeled as links and nodes, and demand is assumed to be concentrated at hypothetical zone centroids. In contrast, a continuum modeling approach, in which the dense transportation network is approximated as a continuum and travel demand is distributed in a continuous manner in the modeling region, has also been used to evaluate the transportation cost for determination of the housing location choice (Ho and Wong, 2007, 2005; Yin et al., 2013). In the continuum modeling approach, model quantities (e.g., travel cost, demand flows) can be represented by a smooth mathematical function (Vaughan (1987)) and are more suitable for macroscopic-level studies (e.g., initial phase of planning/modeling) and for modeling environmental factors/effects (e.g., air pollutants) (Ho and Wong, 2007; Yang et al., 2019). Thus, Ho and Wong (2007) and Yin et al. (2013) adopted a logit-based location choice model that is continuously defined over the modeling region and, is dependent upon transportation and housing rent to model travelers' housing-location choice.

Comparing to the discrete modelling approach, the continuum model approach has the following benefits (Blumenfeld, 1977; Taguchi and Iri, 1982; Sasaki et al., 1990; Gwinner, 1998; Ho and Wong, 2006; Yin et al., 2013, 2017). First, the continuum modeling approach reduces the problem size in modeling a dense transportation network as it approximates the region as a continuum instead of modeling each of the links/nodes as in the discrete modeling approach. Second, as it is not required to defines each of the links/nodes in the modeled region as for the discrete modeling approach, the continuum approach requires less data for model building and is more suitable for initial-stage planning as data availability is limited. Third, as no links and

nodes are considered, the continuum modeling approach focus more on the trends and patterns that leads to a better understanding of various global characteristics (e.g., travel demand, land development intensity, travel cost, etc.) of the modeling region. Fourth, in traffic analysis, not all the analyzed quantities could be reasonably defined in links and nodes as required in the discrete modeling approach. For example, despite the emissions of air pollutants are from vehicles traveling on roads/links, the dispersions of these air pollutants are continuous over the whole city (e.g., disperse to the residential/commercial area) (Stockie, 2011). In such case, the continuum models could directly and precisely model those continuously varied quantities (e.g., concentration of air pollutants) and incorporate them into the analysis.

In addition to the housing and transportation costs discussed in the previous paragraphs, recently, there is increasing concerns in considering environmental factors, especially air quality, in determining the housing location-choices of consumers/travelers (Wardman and Bristow, 2004; Wagner and Wegener, 2007; Bednar et al., 2011). Newman and Kenworthy (1989) studied the land use, transport infrastructure, private transport, and public transport data for 1980 and 1990 in a global sample of cities (excluding the developing Asian cities), and found that residential density is inversely proportional to traffic-related energy consumption. Sullivan (2017) has provided evidence showing that clean air has a much higher social value than previously believed. Liu et al. (2018) studied the impacts of haze on housing prices, and found that haze has significant negative impacts on both selling and rental prices of houses. It also found that housing rental prices have a more significant response to the air quality than that for housing sale prices. Wagner and Wegener (2007) introduced the ILUMASS model that considers the impact of transport-related emissions on the residential location and for workplace location. Furthermore, Wardman and Bristow (2004) and Bednar et al. (2011) developed various emission-sensitive location choice models for empirical and policy studies. Various emission models have been considered for accurate estimation of transport-related emissions. Emission factor models (CARB, 2006) and physical power-demand models (Scora and Barth, 2006) are common approaches for modeling transport-related emissions. However, these approaches suffer from the deficiencies of neglecting vehicle-operating states and the driving environment, and lack detailed information of vehicle operation characteristics for precise estimation of vehicular emissions (Yin et al. (2013)). To resolve these problems, models based on acceleration and speed, in which the emission rate depends upon the vehicle type and instantaneous speed and acceleration, have been widely considered in the literature (Ahn et al., 1999; Rakha et al., 2004). Owing to the continuous nature of the model parameters and variables, a continuum modeling approach is required to model vehicular emissions in the transportation network and their effect on the choice of housing location (Yin et al., 2013). As the emitted pollutants will disperse, the use of an emission model alone is not sufficient to precisely model the spatial and temporal variation in the pollutant concentrations. Thus, a Gaussian dispersion model (Yin et al., 2017) and a three-dimensional advection-diffusion equation (Yang et al., 2019) have been used in recent studies to model the concentration of air pollutants more realistically.

In the studies of housing-location choice with the continuum modeling approach, the dispersion of air pollutants is either not considered (Yin et al., 2013) or is only statically modeled (Yin et al., 2017). However, the temporal dispersion of air pollutants is crucial in defining the environmental index for housing location choice and should be precisely addressed. In addition, the emission model (Ahn et al., 1999) used in previous studies (Yin et al., 2013, 2017; Yang et al., 2019) is only a microscopic emission model and should be extended to macroscopic level to consist with the adopted continuum network model. To address these issues, this study adopted a dynamic continuum-modeling version of the traffic equilibrium problem to study the effects of the transportation cost, housing rent, and air quality on the choice of housing location in an urban city with multiple central business districts (CBDs). In this study, a macroscopic emission model and a time-dependent dispersion model were used to realistically model the spatial and temporal variation in emitted pollutants. The traffic flows and, thus, the transportation costs in this study were determined by the predictive continuum dynamic user-optimal (PDUO-C) model with consideration of departure-time choice. Based on the transportation cost (from PDUO-C), the perceived air quality (from PDUO-C and emis-

sion/dispersion model), and housing rent, a housing-location model was formulated and solved to determine the housing location of the travelers in the continuum modeling area.

This study has the following three contributions. First, this study has adopted a dynamic model (i.e., PDUO-C model) to study the housing location choice with consideration of the impacts from air quality. Dispersion of the emitted air pollutants, which is highly time dependent, could be more realistically modeled under this dynamic framework and provide a more reasonable concentration of air pollutants (or air quality) for travelers/citizens in deciding their housing locations. Second, this study extends the microscopic emission model adopted in Yang et al. (2019) to macroscopic emission model to ensure the consistence with the macroscopic nature of the adopted PDUO-C model. Third, this study extends the PDUO-C model (Du et al., 2013; Lin et al., 2018) to incorporate the complete day demands (or traffic flows), which includes trips from home to CBD in the morning and trips from CBD back to home in the evening, within the modeling region. This extension aims to provide a complete evaluation of travel costs considered in housing location choice.

The paper is organized as follows. Section 2 gives the formulation of the housing-location choice problem based on the PDUO-C model with consideration of departure-time choice and the emission/dispersion of air pollutants. Solution algorithms to solve the PDUO-C model and housing location choice model are introduced in Section 3. Section 4 uses a numerical example to demonstrate the characteristics of this model and the effectiveness of the solution algorithm. Finally, conclusions of this study are given in Section 5.

2 Model formulation

To facilitate the presentation of essential ideas, the following assumptions are adopted in this paper:

A1. The proposed model falls in the category of continuum modeling approach for network equilibrium problem. Road network considered in this study is relatively dense and is approximated as a continuum. Travelers (or vehicles) are free to travel in both x and y

- direction within the modeling region (Ho and Wong, 2005, 2007; Du et al., 2013; Yang et al., 2019).
- A2. Travelers have perfect information about traffic conditions (e.g., flows, travel times, etc.) over time and is familiar with the modeling region (Du et al., 2013; Lin et al., 2018).
- A3. Only trips from travelers' home location to CBDs, or from the CBDs back to their home location, are considered in this study (Lin et al., 2018; Yang et al., 2019). Other trips (e.g., trips between home locations of different travelers) are ignored in this study.
- A4. The modeling period (T) covers a complete day and is divided into 2 sub-periods: T_1 and T_2 . During T_1 , all travelers travel from their home locations to CBDs and there are no traveler leaving the CBDs. During T_2 , all travelers travel from CBDs back to their home locations and there are no traveler traveling to the CBD (Yang et al., 2019).
- A5. Variations of topography within the modeling region are negligible and the ground surface (i.e., z = 0) can be taken as the plane (Stockie, 2011; Yang et al., 2019).
- A6. Air pollutants from transport-related emission are emitted from a surface source at ground surface (i.e., z = 0) (Stockie, 2011; Yang et al., 2019).

In this study, an urban city of arbitrary shape and with multiple CBDs (Figure 1) is considered as the modeling region, and the road network outside the CBDs is assumed to be relatively dense and able to be approximated as a continuum. Let the modeling region be Ω and the outer boundary be Γ_o . The boundary of each CBD is denoted by Γ_c^m , $\forall m \in \{1, ...M\}$, which M is the number of CBDs in the modeling region. Then, let $\Gamma = \Gamma_o \cup (\cup_m \Gamma_c^m)$ be the boundary of Ω . In this study, travelers are classified into M groups depending on the CBD to which they are traveling. Note that for group m travelers, CBDs other than their destination (i.e., the m-th CBD) are considered as obstacles around which they must detour.

Let $v^m = (v_1^m(x, y, t), v_2^m(x, y, t))$ be the velocity vector of group m travelers at location $(x, y) \in \Omega$ at time $t \in T^j$, which $v_1^m(x, y, t)$ and $v_2^m(x, y, t)$ are respectively the speeds in the x

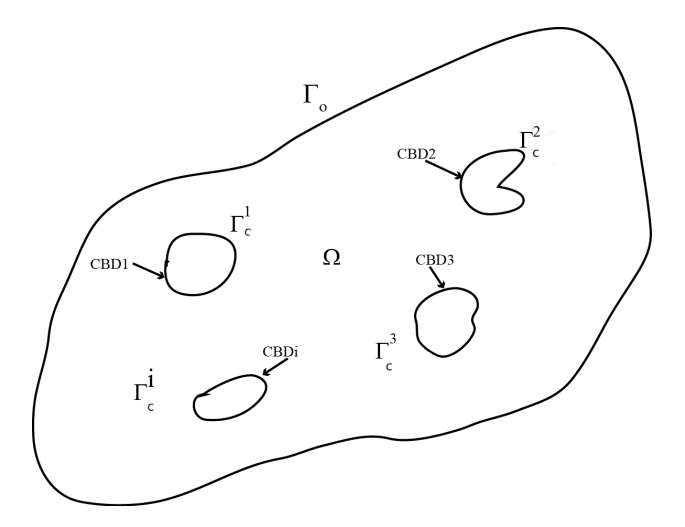


Fig. 1: An example of a modeling domain

and y directions. $T^j = [t^j_{beginning}, t^j_{end}]$ denotes the j-th modeling period with $t^j_{beginning}$ and t^j_{end} are respectively the time for modeling period j to begin and end, and J is the number modeling period. In this study, J = 2 (i.e., $j \in \{1,2\}$) and denotes $T = T^1 \cup T^2$, which T^1 and T^2 are respectively the modeling period for traffic traveling from home locations to CBDs and from CBDs back to home locations, to represent the complete time period for modeling. Define $V^m(x,y,t)$ as the speed (in km/h) of group m travelers at location $(x,y) \in \Omega$ at time $t \in T^j$, which is the norm of the corresponding velocity vector (i.e., $V^m = |v^m|$), and is defined as:

$$V^{m}(x, y, t) = V_{f}^{m} e^{-\zeta (\sum_{m=1}^{M} \rho^{m})^{2}}, \quad \forall (x, y) \in \Omega, \ t \in T^{j},$$
 (1)

where $V_f^m(x,y)$ (in km/h) is the free-flow speed of group m travelers at location $(x,y) \in \Omega$, $\rho^m(x,y,t)$ (in veh/km^2) is the density of group m travelers at location $(x,y) \in \Omega$ at time $t \in T^j$, $\zeta(x,y)$ (in km^4/veh^2) is a positive scalar at location $(x,y) \in \Omega$ and should be exogenously defined based on the corresponding road condition. As different groups of travelers are traveling in different directions to their destination, there would be different speeds, which depends on the direction of travel (or traveler's group), at the same location (x,y) and time (t). Flow vector of group m travelers at location $(x,y) \in \Omega$ at time $t \in T^j$ is denoted by $f^m = (f_1^m(x,y,t), f_2^m(x,y,t))$ with $f_1^m(x,y,t)$ and $f_2^m(x,y,t)$ are respectively the flow fluxes in the x and y directions. This flow vector is depended on the density and velocity vector of the

corresponding location and time, and is defined by the following equation:

$$\mathbf{f}^m = \rho^m \mathbf{v}^m, \quad \forall (x, y) \in \Omega, \quad t \in T^j$$
 (2)

With Equation (2) and the definition of velocity vector, the corresponding flow intensity (i.e., norm of the flow vector) is defined as $|f^m| = \rho^m V^m$. The local travel cost per unit distance of travel (in \$/km) at location $(x,y) \in \Omega$ at time $t \in T^j$ for group m travelers is denoted by $c^m(x,y,t)$ and has the following functional relationship:

$$c^{m}(x, y, t) = \frac{\kappa}{V^{m}} + \pi \left(\sum_{m=1}^{M} \rho^{m}\right), \quad \forall (x, y) \in \Omega, \ t \in T^{j}$$
(3)

where κ is the value of time. The first term on the RHS of Equation (3) represents the cost related to travel time. The second term in Equation (3) represents other costs that depend on vehicle density, for example, congestion pricing (Ho and Wong, 2005) and the cost of discomfort due to crowding (Hoogendoorn and Bovy, 2004). The total travel cost of group m travelers at location $(x, y) \in \Omega$ traveling to/from the m-th CBD, $l^m(x, y, t)$, is defined as:

$$l^{m}(x, y, t) = p^{m}(x, y, t) + \phi^{m}(x, y, t)$$
(4)

where $\phi^m(x,y,t)$ is the actual travel cost potential (or simply actual travel cost) of group m travelers depart from their home location (x,y) at time $t \in T^1$ and use the constructed path-choice strategy to the m-th CBD (i.e. going to work). For departure time $t \in T^2$, $\phi^m(x,y,t)$ denotes the actual travel cost potential of group m travelers depart from m-th CBD to travel to their home location (x,y) (i.e. back to home). $p^m(x,y,t)$ is the schedule delay cost of group m travelers departing from location (x,y) at time t and traveling to the m-th CBD (or in the reverse direction). Such schedule delay cost is defined as penalty for late and early arrival, and is determined by the arrival time: $t + I^m(x,y,t)$, which $I^m(x,y,t)$ denotes the travel time of group m travelers departing from location (x,y) at time t and traveling to the m-th CBD (or in the reverse direction). The details of schedule delay cost, $p^m(x,y,t)$, will be discussed in Section 2.2. With the cost potential $\phi^m(x,y,t)$, average transportation cost between location (x,y) and the m-th CBD (group m travelers), $\Phi^m(x,y,t)$, is defined as:

$$\Phi^{m}(x,y) = \frac{1}{|T^{1}|} \int_{T^{1}} \phi^{m}(x,y,t)dt + \frac{1}{|T^{2}|} \int_{T^{2}} \phi^{m}(x,y,t)dt.$$
 (5)

The average transportation cost in Equation (5) is used to defined the total perceived travel cost between location (x, y) and the m-th CBD (group m travelers), $P^m(x, y)$:

$$P^{m}(x, y) = \theta^{m} + S^{m}(Q^{m}) + \Phi^{m}(x, y)$$
(6)

where θ^m is the parameter representing travelers' preference for the *m*-th CBD; $S^m(Q^m)$ is the internal operating cost of traffic (e.g., parking cost, local circulation cost, etc) within the *m*-th CBD and is depended on the total travel demand attracted to that CBD, Q^m :

$$Q^{m} = \int_{T_{i}} \int_{\Omega} \bar{q}^{m}(x, y, t) d\Omega. dt$$
 (7)

which $q^m(x,y,t)$ (in $veh/km^2/h$) is the travel demand of group m travelers at location (x,y) at time t. Based on $q^m(x,y,t)$, the travel demand of group m travelers at location (x,y) in modeling period j is defined as $q^{mj}(x,y) = \int_{T^j} q^m(x,y,t) dt$.

With the above fundamental definitions, the formulation of various models adopted in this study are introduced in the following sub-sections. The Figure 2 shows the interrelationship of the models introduced in Section 2. With a given distribution of travel demands, the dynamic user-optimal model with departure-time consideration (Section 2.3), which make use of the PDUO-C model (Section 2.1) and schedule delay cost (Section 2.2), will solve for total perceived travel cost and time-dependent speeds over the modeling region. The estimated time-dependent speeds will be used in the emission model (Section 2.4) for determining the amount of emitted air pollutants. The dispersion of these emitted air pollutants will be modeled in Section 2.5 for determining the corresponding concentrations over the modeling region. With these concentrations of air pollutant and total perceived travel costs from Section 2.3, the housing location choice model (Section 2.6) will determine the housing location choices of the travelers and, thus, the distribution of travel demands.

2.1 Predictive continuum dynamic user-optimal model

In this study, for modeling the emission and dispersion of air pollutants in a more realistic manner, the predictive continuum dynamic user-optimal model (PDUO-C) is adopted. PDUO-C governs the route-choice behavior of the multiple-group travelers, which will lead to the

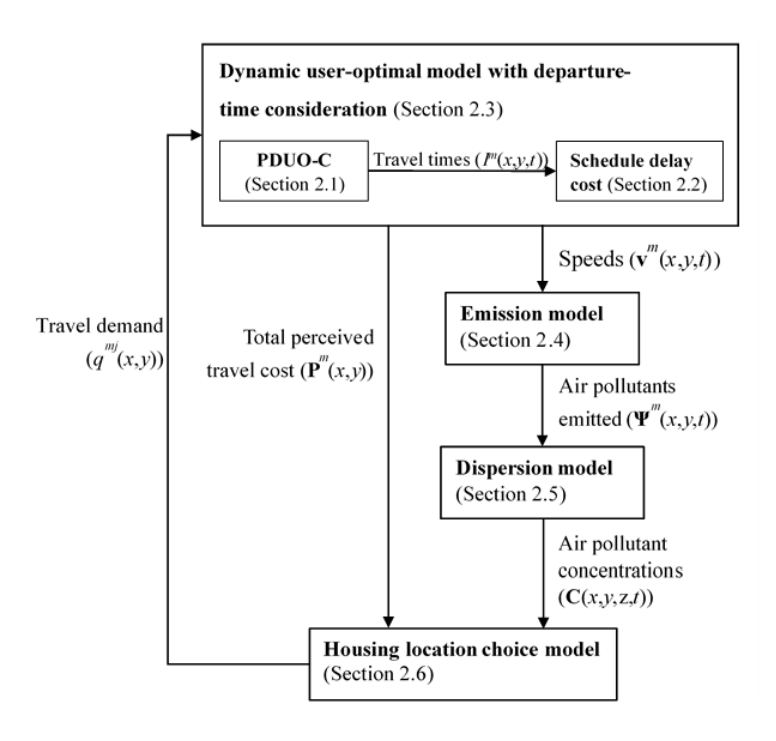


Fig. 2: The flowchart of the proposed housing location choice model.

emission and dispersion of air pollutants, in the various modeling periods. For a more-detailed discussion of the formulation of PDUO-C models, readers are referred to Du et al. (2013) and Lin et al. (2018). To further extend the previous PDUO-C models to incorporate demands in complete day, the PDUO-C model adopted in this study is separately defined for: i) travelers traveling to the CBDs (j = 1) and ii) travelers traveling from the CBDs (j = 2). For the first modeling period (i.e., j = 1) the conservation laws, which govern the densities of travelers ($\rho^m(x, y, t)$), and the Hamilton-Jacobi equation, which governs the cost potentials ($\phi^m(x, y, t)$), are defined in Equations (8) and (9) below:

$$\begin{cases}
\rho_t^m(x,y,t) + \nabla \cdot \boldsymbol{f}^m(x,y,t) = q^m(x,y,t) & \forall (x,y) \in \Omega, t \in T^1, m \in \{1,\dots,M\} \\
\boldsymbol{f}^m(x,y,t) = -\rho^m(x,y,t)V^m(x,y,t)\frac{\nabla \phi^m(x,y,t)}{|\nabla \phi^m(x,y,t)|} & \forall (x,y) \in \Omega, t \in T^1, m \in \{1,\dots,M\} \\
\boldsymbol{f}^m(x,y,t) \cdot \boldsymbol{n}(x,y) = 0 & \forall (x,y) \in \Gamma \setminus \Gamma_c^m, t \in T^1, m \in \{1,\dots,M\} \\
\rho^m\left(x,y,t_{beginning}^1\right) = \rho_0^m(x,y) & \forall (x,y) \in \Omega, m \in \{1,\dots,M\}
\end{cases}$$
(8)

$$\begin{cases} \frac{1}{V^{m}(x,y,t)}\phi_{t}^{m}(x,y,t) - |\nabla\phi^{m}(x,y,t)| = -c^{m}(x,y,t) & \forall (x,y) \in \Omega, t \in T^{1}, m \in \{1,\dots,M\} \\ \phi^{m}(x,y,t) = \phi_{CBD}^{m} & \forall (x,y) \in \Gamma_{c}^{m}, t \in T^{1}, m \in \{1,\dots,M\} \\ \phi^{m}(x,y,t_{end}^{1}) = \phi_{0}^{m,1}(x,y) & \forall (x,y) \in \Omega, m \in \{1,\dots,M\} \end{cases}$$
(9)

where $\rho_t^m(x,y,t) = \partial \rho^m(x,y,t)/\partial t$, $\nabla \cdot \boldsymbol{f}^m(x,y,t) = (\partial f_x^m(x,y,t)/\partial x) + (\partial f_y^m(x,y,t)/\partial y)$, and $\phi_t^m(x,y,t) = \partial \phi^m(x,y,t)/\partial t$; $\boldsymbol{n}(x,y)$ is the unit normal vector pointing outward from the boundary; ϕ_{CBD}^m is the value of ϕ^m on the boundary of the corresponding CBD (i.e., the *m*-th CBD); $\phi_0^{m,1}$ is the initial value of $\phi^m(x,y,t)$ in the first modeling period (i.e., T^1). As only the travelers traveling to a CBD are considered in this study, the densities will be zero at the beginning of the modeling period (i.e., $\rho^m(x,y,t_{beginning}^1) = 0$). $\phi_0^{m,1}$ could be solved by considering the following 2D Eikonal equation (Du et al., 2013) (Equation (10)):

$$\begin{cases}
\left|\nabla\phi_0^{m,1}(x,y)\right| = c^m\left(x,y,t_{end}^1\right) & \forall (x,y) \in \Omega, m \in \{1,\ldots,M\} \\
\phi_0^{m,1}(x,y) = \phi_{\text{CBD}}^m & \forall (x,y) \in \Gamma_c^m, m \in \{1,\ldots,M\}
\end{cases}$$
(10)

Based on the formulation of PDUO-C model for travelers traveling to a CBD above and the transformation of the index/variables (i.e., time index, density of travelers, travel demands, flow vectors, actual travel cost potentials, and local travel costs) for travelers traveling back from a CBD as defined in ?, the corresponding conservation law, Hamilton-Jacobi equation, and 2D Eikonal equation for the second modeling period (i.e., j = 2) are defined as follows (Equations (11) and (12)):

$$\begin{cases}
\rho_t^m(x,y,t) + \nabla \cdot \mathbf{f}^m(x,y,t) = q^m(x,y,t) & \forall (x,y) \in \Omega, t \in T^2, m \in \{1,\dots,M\} \\
\mathbf{f}^m(x,y,t) = \rho^m(x,y,t)V^m(x,y,t)\frac{\nabla \phi^m(x,y,t)}{|\nabla \phi^m(x,y,t)|} & \forall (x,y) \in \Omega, t \in T^2, m \in \{1,\dots,M\} \\
\mathbf{f}^m(x,y,t) \cdot \mathbf{n}(x,y) = 0 & \forall (x,y) \in \Gamma \setminus \Gamma_c^m, t \in T^2, m \in \{1,\dots,M\} \\
\rho^m(x,y,t_{end}^2) = 0 & \forall (x,y) \in \Omega, m \in \{1,\dots,M\}
\end{cases}$$
(11)

$$\begin{cases}
\frac{1}{V^{m}(x,y,t)}\phi_{t}^{m}(x,y,t) - |\nabla\phi^{m}(x,y,t)| = -c^{m}(x,y,t) & \forall (x,y) \in \Omega, t \in T^{2}, m \in \{1,\dots,M\} \\
\phi^{m}(x,y,t) = \phi_{CBD}^{m} & \forall (x,y) \in \Gamma_{c}^{m}, t \in T^{2}, m \in \{1,\dots,M\} \\
\phi^{m}(x,y,t_{begining}^{2}) = \phi_{0}^{m,2}(x,y) & \forall (x,y) \in \Omega, m \in \{1,\dots,M\}
\end{cases}$$
(12)

 $\phi_0^{m,2}$ could be solved by considering the following 2D Eikonal equation (Equation (13)):

$$\begin{cases}
\left|\nabla\phi_0^{m,2}(x,y)\right| = c^m \left(x, y, t_{begining}^2\right) & \forall (x,y) \in \Omega, m \in \{1, \dots, M\} \\
\phi_0^{m,2}(x,y) = \phi_{CBD}^m & \forall (x,y) \in \Gamma_c^m, m \in \{1, \dots, M\}
\end{cases}$$
(13)

2.2 Schedule delay cost

In this study, travelers will consider the schedule delay cost, which is determined by their desired arrival time, when making their departure time and route choice. Following Du et al.

(2013), the travel time of group m travelers departing from location (x, y) at time t and traveling to the m-th CBD $(I^m(x, y, t))$ is defined as (Equation (14)):

$$|\nabla I^{m}(x, y, t)| = \frac{1}{V^{m}(x, y, t)}, \quad \forall (x, y) \in \Omega, t \in T^{j}, j \in \{1, \dots, J\}, m \in \{1, \dots, M\}$$
 (14)

It is assumed that the desired arrival time period for the m-th group travelers in modeling period j is defined by $\left[t^{mj^*} - \Delta, t^{mj^*} + \Delta\right]$, in which t^{mj^*} denotes the middle of this desire arrival time period and Δ , which is a positive scalar, is a measure of arrival time flexibility. With this desired arrival time period, the schedule delay cost $(p^m(x, y, t))$ is defined as follows (Equation (15)):

$$p^{m}(x, y, t) = \begin{cases} \gamma_{1} \left[\left(t^{mv^{*}} - \Delta \right) - \left(t + I^{m}(x, y, t) \right) \right] & t + I^{m}(x, y, t) < t^{m*} - \Delta, \\ 0 & t^{m*} - \Delta \le t + I^{m}(x, y, t) \le t^{m*} + \Delta, \\ \gamma_{2} \left[\left(t + I^{m}(x, y, t) \right) - \left(t^{my^{*}} + \Delta \right) \right] & t + I^{m}(x, y, t) > t^{m*} - \Delta, \end{cases}$$
(15)

where γ_1 and γ_2 are both positive scalar and are respectively the values of time for early and late arrival. According to previous empirical studies, it is assumed that $\gamma_2 > \kappa > \gamma_1$, which κ is the value of time as used in Equation (??). With the above definition of schedule delay cost ($p^m(x, y, t)$), the total travel cost ($l^m(x, y, t)$) could be calculated by Equation (4).

2.3 Dynamic user-optimal model with departure time consideration

With the PDUO-C model (Section 2.1), the traffic flow ($f^m(x, y, t)$) and thus the total travel cost ($l^m(x, y, t)$) within the modeling region could be obtained with a given the distribution of travel demand, $q^m(x, y, t)$. As the total travel cost is dependent on the travel demands, denote $l^m(x, y, t) = l^m(x, y, t, q^j)$ with $q^j = \{q^m(x, y, t), \forall (x, y) \in \Omega, t \in T^j, m = 1, ..., M\}$. Let $\hat{l}^{mj}(x, y, q^j)$ be the minimum of total travel cost of group m travelers at location (x, y) in modeling period j and is defined by the following equation (Equation (16)):

$$\hat{l}^{mj}(x, y, q^j) = \operatorname{ess\,inf} \left\{ l^m(x, y, t, q^j), \quad \forall t \in T^j \right\},\tag{16}$$

Definition 2.1. The dynamic user-optimal with departure-time consideration is satisfied in the modeling period j if the following equation is satisfied (Equation (17)):

$$\begin{cases}
l^{m}(x,y,t,q^{j}) = \hat{l}^{mj}(x,y,q^{j}), & \text{if } q^{m}(x,y,t) > 0 \\
l^{m}(x,y,t,q^{j}) \ge \hat{l}^{mj}(x,y,q^{j}), & \text{if } q^{m}(x,y,t) = 0
\end{cases}$$
(17)

where $\Lambda^j = \left\{ \mathbf{q}^j : q^m(x, y, t) \ge 0, \int_{T^j} q^m(x, y, t) dt = q^{mj}(x, y) \forall (x, y) \in \Omega, t \in T^j, m = 1, \dots, M \right\}$ denotes the feasible set of travel demand \mathbf{q}^j .

The dynamic user-optimal condition defined in Equation (17) is to ensure that the total travel cost incurred by travelers who depart at any time is equal and minimized and that no traveler in the system can reduce his or her total travel cost by changing his or her departure time and route choice. With this definition, the variational inequality formulation of dynamic user-optimal with simultaneous consideration of departure time and route choice are defined by the following theorem.

Theorem 2.1. The dynamic user-optimal condition in **Definition 2.1** is equivalent to the following variational inequality problem (Equation (18)) in modeling period j: Find $\mathbf{q}^{j^*} \in \Lambda^j$ so that for all $\mathbf{q}^j \in \Lambda^j$,

$$\sum_{m \in \{1,\dots,M\}} \iint_{\Omega} \int_{T^j} l^m \left(x, y, t, \boldsymbol{q}^{j^*}\right) \left(q^m(x, y, t) - q^{m^*}(x, y, t)\right) dt d\Omega \ge 0$$
(18)

proof. See Appendix A.

Similar to various studies on traffic equilibrium problems (Lin et al. (2018); Long et al. (2015, 2016); Huang et al. (2002)), this study also adopted a gap function to evaluate the equality of numerical solution throughout the solution procedures. In this study, the gap function was taken as follows (Equation (19)):

$$GAP = \sum_{m \in \{1, M\}} \iint_{\Omega} \int_{T^{j}} q^{m}(x, y, t) (l^{m}(x, y, t, \bar{q}^{j}) - \hat{l}^{m}(x, y, \bar{q}^{j})) dt$$
 (19)

Similar to Lin et al. (2018), the above gap function has the properties of i) $GAP \ge 0$ and ii) $GAP = 0 \Leftrightarrow q^j$ is a solution of the variational inequality (VI) problem (Equation 18) and the dynamic user-optimal problem (Equation 17), of the corresponding time period. As the gap function provides a convergence measure of the VI problem (dynamic user-optimal problem), the following relative gap function was adopted as the stopping criterion of the

solution algorithm (Equation (20)):

$$RGAP = \frac{\sum_{m \in \{1,...,M\}} \iint_{\Omega} \int_{T^{j}} q^{m}(x,y,t) (l^{m}(x,y,t,\bar{q}^{j}) - \hat{l}^{mj}(x,y,q^{j})) dt d\Omega}{\sum_{m \in \{1,...,M\}} \iint_{\Omega} q^{mj}(x,y) \hat{l}^{mj}(x,y,q^{j}) d\Omega}$$
(20)

2.4 Emission model

In this study, the residents' housing location choice depended not only on transportation costs, which are determined by the PDUO-C model in the previous section, but also on the air quality of the housing locations. Transport-related emissions are among the major sources of air pollutants that directly affect air quality. Typically, emission models of vehicles are at the microscopic level (i.e., individual vehicle) and are assumed to be dependent on the instantaneous acceleration and speed (Ahn et al. (1999); Yang et al. (2019)) of that vehicle (Equation (21)):

$$\psi^{m}(x, y, t) = \psi^{m}(U^{m}(x, y, t), s^{m}(x, y, t)) \exp\left[\sum_{k=0}^{3} \sum_{k=0}^{3} \omega_{i,k} \left[V^{m}(x, y, t)\right]^{i} \left[s^{m}(x, y, t)\right]^{k}\right]$$
(21)

where $\psi^m(x,y,t)$ (in $kg/(veh\ h)$) is the amount of air pollutants generated per hour per vehicle used by traveler group m at location (x,y) at time t; $U^m(x,y,t)$ (in km/h) is the instantaneous speed of the vehicle used by traveler group m at location (x,y) at time t; $s^m(x,y,t)$ (in km/h^2) is the instantaneous acceleration of vehicle used by traveler group m at location (x,y) at time t; ω_{ik} is the model regression coefficient for speed power i and acceleration power k and differs for various kinds of emissions (e.g., HC, CO, or NO_x). To ensure the consistency of adopted emission model with the PDUO-C model – which defines traffic flows, speeds, and accelerations of vehicles at macroscopic level – a macroscopic emission model will be derived from the above microscopic emission model (Equation (21)). To derive the macroscopic emission model, it is first assumed that the instantaneous speed ($U^m(x,y,t)$) and instantaneous acceleration ($s^m(x,y,t)$) are random variables that follow certain normal distributions (i.e., $U^m(x,y,t) \sim N(V^m(x,y,t),\sigma_V^m)$ and $s^m(x,y,t) \sim N(a^m(x,y,t),\sigma_a^m)$) (Leong, 1968; McLean, 1989; Dey and Gangopadhaya, 2006; Viti et al., 2008). $V^m(x,y,t)$ and $a^m(x,y,t)$ (σ_V^m and σ_a^m) are the mean (standard deviation) of the distributions of instantaneous speed and instantaneous

acceleration, respectively, at the corresponding location and time. Application of the Taylor series expansion to Equation (21) up to the second-order term could show that (Equation (22)):

$$\psi^{m}(U^{m}, s^{m}) \approx \psi(V^{m}, a^{m}) + \frac{\partial \psi(V^{m}, a^{m})}{\partial U^{m}} (U^{m} - V^{m}) + \frac{\partial \psi(V^{m}, a^{m})}{\partial s^{m}} (s^{m} - a^{m})$$

$$+ \frac{1}{2} \frac{\partial^{2} \psi(V^{m}, a^{m})}{\partial (U^{m})^{2}} (U^{m} - V^{m})^{2} + \frac{1}{2} \frac{\partial^{2} \psi(V^{m}, a^{m})}{\partial (s^{m})^{2}} (s^{m} - a^{m})^{2}$$

$$+ \frac{\partial^{2} \psi(V^{m}, a^{m})}{\partial U^{m} \partial s^{m}} (U^{m} - V^{m}) (s^{m} - a^{m})$$

$$(22)$$

where the x, y, and t indices of variables U^m , s^m , V^m and a^m are omitted for simplicity. $E(U^m - V^m) = 0$, $E(s^m - a^m) = 0$, $E((U^m - V^m)^2) = (\sigma_V^m)^2$, $E((s^m - a^m)^2) = (\sigma_a^m)^2$ and $E((U^m - V^m)(s^m - a^m)) = 0$, with $E(\cdot)$ denotes the expected value, and the fact that $\psi^m(V^m, a^m)$ is independent on U^m and s^m , the expected value of $\psi^m(U^m, s^m)$, $\Psi^m(x, y, t)$, is defined as (Equation (23)):

$$\Psi^{m}(x, y, t) = E(\psi^{m}(U^{m}, s^{m})) \approx \psi(V^{m}, a^{m}) + \frac{1}{2} \frac{\partial^{2} \psi(V^{m}, a^{m})}{\partial (U^{m})^{2}} (\sigma_{V}^{m})^{2} + \frac{1}{2} \frac{\partial^{2} \psi(V^{m}, a^{m})}{\partial (s^{m})^{2}} (\sigma_{a}^{m})^{2}$$
(23)

where $\frac{\partial^2 \psi(V^m, a^m)}{\partial (U^m)^2}(\sigma_V^m)^2$ and $\frac{\partial^2 \psi(V^m, a^m)}{\partial (s^m)^2}(\sigma_a^m)^2$ could be determined by direct differentiation from Equation (22). Note that $\Psi^m(x, y, t)$ defined in Equation (23) is the macroscopic emission model group m travelers. V^m and a^m in Equation (23) could be obtained from the PDUO-C model, while σ_V^m and σ_a^m are externally determined. Under PDUO-C route choice behavior, travelers' vehicles will accelerate or decelerate along their chosen route based on the traffic conditions. Acceleration ($a^m(x, y, t)$) is defined as follows (Equation (24)):

$$a^{m}(x,y,t) = \frac{a_{1}^{m}(x,y,t)\phi_{x}^{m}(x,y,t) + a_{2}^{m}(x,y,t)\phi_{y}^{m}(x,y,t)}{\sqrt{\left[\phi_{x}^{m}(x,y,t)\right]^{2} + \left[\phi_{y}^{m}(x,y,t)\right]^{2}}}$$
(24)

where $a_1^m(x, y, t)$ and $a_2^m(x, y, t)$ are the accelerations in the x and y directions, respectively, at location (x, y) at time t, $\phi_x^m(x, y, t) = \partial \phi^m(x, y, t)/\partial x$ and $\phi_y^m(x, y, t) = \partial \phi^m(x, y, t)/\partial y$. $a_1^m(x, y, t)$ and $a_2^m(x, y, t)$ are further defined as (Equations(25) and (26)):

$$a_1^m(x, y, t) = \frac{\partial v_1^m(x, y, t)}{\partial t} + v_1^m(x, y, t) \frac{\partial v_1^m(x, y, t)}{\partial x} + v_2^m(x, y, t) \frac{\partial v_1^m(x, y, t)}{\partial y}$$

$$\forall (x, y) \in \Omega, t \in T^j, j \in \{1, \dots, J\}, m \in \{1, \dots, M\} \quad (25)$$

$$a_2^m(x,y,t) = \frac{\partial v_2^m(x,y,t)}{\partial t} + v_1^m(x,y,t) \frac{\partial v_2^m(x,y,t)}{\partial x} + v_2^m(x,y,t) \frac{\partial v_2^m(x,y,t)}{\partial y}$$

$$\forall (x, y) \in \Omega, t \in T^j, j \in \{1, \dots, J\}, m \in \{1, \dots, M\}$$
 (26)

Although there are no single representative measures for traffic-related air pollution, this study adopts NOx as the indicative measure given its infamous adverse health effects (Wardman and Bristow (2004)). To define the NO_x emissions through Equation (21), the required coefficients (ω_{ik}) were given by Ahn et al. (1999) and Yang et al. (2019). For other pollutants, the corresponding coefficient could also be found in Ahn et al. (1999).

2.5 Dispersion model

Air pollutants from transport-related emissions, which are defined in Section 2.4, and other sources (e.g., pollutants emitted from power plants and from residents' activities in the CBD), will disperse via turbulent diffusion and wind advection. Concentration of any air pollutant, C(x, y, z, t), is defined by the following three-dimensional advection-diffusion equation (Equation (27)):

$$\frac{\partial C(\cdot)}{\partial t} + \nabla \cdot \left(C(\cdot) u_f(\cdot) \right) = \frac{\partial}{\partial x} \left(K_x \frac{\partial C(\cdot)}{\partial x} \right) + \frac{\partial}{\partial y} \left(K_y \frac{\partial C(\cdot)}{\partial y} \right) + \frac{\partial}{\partial z} \left(K_z \frac{\partial C(\cdot)}{\partial z} \right) + \hat{S}(\cdot) \tag{27}$$

where $\widehat{\Omega}$ is the dispersion region; $C(\cdot) = C(x,y,z,t)$ (in kg/km^3) is the concentration of any air pollutant at location (x,y,z) at time t with z represents the height about ground. $K_x(\cdot) = K_x(x,y,z,t), K_y(\cdot) = K_y(x,y,z,t), K_z(\cdot) = K_z(x,y,z,t)$ (in km^2/h) are respectively the eddy diffusivities in x, y and z directions. These eddy diffusivities are assumed to be location and time dependent to account for the different dispersion characteristics due to built environment and time (Pasquill, 1961; Whaley, 1974; Stockie, 2011). $\hat{S}(\dot{j} = \hat{S}(x,y,z,t) = \hat{S}_0(x,y,z,t) + \hat{S}_t(x,y,z,t)$ (in kg/km^3h) is the source term defining the source of air pollutant (i.e., C(x,y,z,t)) at location (x,y,z) at time t, where $\hat{S}_t(x,y,z,t)$ represents the air pollutants from traffic, and $\hat{S}_0(x,y,z,t)$ represents air pollutants from other sources (e.g., power plants, residents' activities). The source term, $\hat{S}_0(x,y,z,t)$ and $\hat{S}_t(x,y,z,t)$ is defined as (Equations (28) and (29)):

$$\hat{S}_{t}(x, y, z, t) = \delta(z) \sum_{m \in \{1, \dots, M\}} \rho^{m}(x, y, t) \Psi^{m}(x, y, t) \quad \forall (x, y, z) \in \tilde{\Omega}, t \in T^{j}, j \in \{1, \dots, J\}$$
 (28)

$$\hat{S}_0(x, y, z, t) = \delta(z)\tilde{\psi}(x, y, t) \tag{29}$$

where $\delta(z)$ (in km^{-1}) is the Dirac delta function, and $\tilde{\psi}(x, y, t)$ (in $kg/(km^2 h)$) is the emission rate of sources other than traffic.

2.6 Housing location choice model

This study, in addition to the housing rent and travel costs that have been considered in most previous studies, also considers the externalities of CBDs and local air quality as the criteria for travelers in making their housing (home) location choice. The housing location choice problem of travelers is governed by the following travel demand distribution function (Equation (30)):

$$q(x,y) = Q \frac{\exp(-\hat{\gamma}\sigma(x,y))}{\iint_{\Omega} \exp(-\hat{\gamma}\sigma(x,y))d\Omega}, \quad \forall (x,y) \in \Omega$$
 (30)

$$\sigma(x,y) = \Pi(x,y) + \tau(x,y) + r(x,y), \quad \forall (x,y) \in \Omega$$
 (31)

where $\Pi(x, y)$ is the log-sum of total perceived travel costs of location (x, y) to all CBDs and is defined as follows (Equation (32)):

$$\Pi(x,y) = -\frac{1}{\chi} \ln \left[\sum_{m \in [1,\dots,M]} \exp\left(-\chi P^m(x,y)\right) \right], \quad \forall (x,y) \in \Omega$$
 (32)

where χ is the sensitivity parameter of the traveler to the total perceived travel cost. $\tau(x, y)$ is the travelers' perception of air quality, which is assumed to have a linear relationship with the

average local pollutant concentration ($\bar{C}(x, y, 0)$), and is defined by Equation (33):

$$\tau(x, y) = \xi \overline{C}(x, y, 0), \quad \forall (x, y) \in \Omega$$
 (33)

where ξ is the unit cost of pollutant concentration, and $\overline{C}(x, y, 0) = \frac{1}{|T|} \int_T C(x, y, 0, t) dt$ is the average local pollutant concentration at location (x, y) and height equals to zero. r(x, y) is the housing rent at location (x, y) and is defined by Equation (34):

$$r(x,y) = \alpha(x,y) \left(1 + \frac{\beta(x,y)q(x,y)}{H(x,y) - q(x,y)} \right), \quad \forall (x,y) \in \Omega$$
 (34)

where H(x,y) is the total housing-supply density at location (x,y) and should be greater than q(x,y); $\alpha(x,y)$ is the perception of housing rents at location (x,y); $\beta(x,y)$ is the scalar parameter that represents the demand-dependent components of the rent function at location (x,y). With the current formulation, it is flexible to adopt different functional form (e.g., higher order polynomial) as the utility function of the logit-based housing location choice model (Equation (31)). Without any further study on the performance of different functional from, this study adopted the simplest and previously adopted (Yin et al., 2013, 2017) functional form (i.e., linear) for combining the impacts of transportation cost, air quality and rent in housing location choice. Equation (30) defines the travel demand at location (x,y), q(x,y), the corresponding proportion of travelers in choosing CBD m (i.e., group m travelers), $q^{mj}(x,y)$, is governed by the following logit-type distribution (Equation (35)):

$$q^{mj}(x,y) = q(x,y) \frac{\exp(-\chi P^m(x,y))}{\sum_{i \in \{1,m\}} \exp(-\chi P^i(x,y))}, \quad \forall (x,y) \in \Omega, j \in \{1,2\}, m \in \{1,\dots,M\}$$
 (35)

with $q(x, y) = \sum_{m \in \{1, ..., M\}} q^{mj}(x, y)$. In addition to the choice of housing location, travel demand $(q^m(x, y, t))$ is also dependent upon the choice of departure time and could be defined by Equation (36):

$$q^{m}(x, y, t) = q^{m}(x, y)g^{m}(x, y, t), \quad \forall (x, y) \in \Omega, t \in T^{j}, j \in \{1, 2\}, m \in \{1, \dots, M\}$$
 (36)

where $g^m(x, y, t)$ is the departure-time distribution at (x, y) within period j and $\int_{T^j} g^m(x, y, t) dt = 1$. In Section 2.3, $q^{mj}(x, y)$ is fixed to find a $g^m(x, y, t)$, or $q^m(x, y, t)$, that satisfies the dynamic user-optimal condition with departure-time consideration. In contrast, this section aims to find a desired $q^{mj}(x, y)$ for a fixed $g^m(x, y, t)$.

3 Solution algorithm

3.1 A projection method for the PDUO-C model with departure-time consideration

In this study, the Lax-Friedrichs scheme is adopted as the numerical approach to discretize and solve the conservation laws (Equations (8) and (11)) and Hamilton-Jacobi equation (Equations (9) and (12)) defined for the PDUO-C model with consideration of departure time. In contrast, the fast-sweeping method is adopted to solve the 2D Eikonal equation (Equations (10) and (13)), which is used to solve for the boundary condition of cost potential (e.g., $\phi_0^{m,1}(x,y)$). The details of using the Lax-Friedrichs scheme and the fast-sweeping method to solve the conservation laws, Hamilton-Jacobi equation, and 2D Eikonal equation could be found in (Du et al., 2013). With the above spatial and temporal discretization, the VI problem (Equation (18)) could be transformed into its discrete form defined by the following equation (Equation (37)):

$$\sum_{1 \le m \le M} \sum_{1 \le i \le N_x} \sum_{1 \le j \le N_y} \sum_{1 \le n \le N_t} l_{ik}^{mm} \left(\tilde{\boldsymbol{q}}^{j^*} \right) \left(q_{ik}^{mn} - q_{ik}^{mn^*} \right) \Delta x \Delta y \Delta t \ge 0 \tag{37}$$

where N_x and N_y are the number of grid points in the x and y directions, respectively, under the proposed discretization; N_t^j are the number of grid points in t direction for modeling period j; $l_{ik}^{mm}\left(\tilde{q}^{j^*}\right)\left(q_{ik}^{mn} \text{ and } q_{ik}^{mn^*}\right)$ represents the value of $l^m(x,y,t,q^{j^*})\left(q^m(x,y,t) \text{ and } q^{m^*}(x,y,t)\right)$ for grid point (i,k,n); $\tilde{q}^{j^*}=\left\{q_{ik}^{mn^*}\forall i=1,\ldots,N_x,k=1,\ldots,N_y,n=1,\ldots,N_t^j,m=1,\ldots,M\right\}$; Δx and Δy are the grid size in the x and y directions, respectively; Δt is the time step and should be chosen to satisfy the Courant–Friedrichs–Lewy condition. Noted that under the discretization in Equation (37) the feasible set of travel demand $(\tilde{\Lambda}^j)$ will also adopt its discrete form (Equation (38)):

$$\tilde{\Lambda}^{j} = \{ \tilde{q} : q_{ik}^{mn} \ge 0, \sum_{n \in \{1, \dots, N_t\}} q_{ik}^{mm} = q_{ik}^{m}$$

$$\forall i = 1, \dots, N_x, k = 1, \dots, N_y, n = 1, \dots, N_t^{j}, m = 1, \dots, M \}$$
(38)

where q_{ik}^m is the total travel-demand of group m travelers at grid point (i, k). In this study, the projection method is adopted to solve the discretized VI problem (Equation (37)) by consider-

ing the following theorem.

Theorem 3.1. Let $\lambda > 0$, \tilde{q}^j is a solution to the discretized VI problem (equation (37)) if and only if (Equation (39))

$$\tilde{\mathbf{q}}^{j*} = P_{\tilde{\Lambda}}(\tilde{\mathbf{q}}^{j*} - \lambda \tilde{\mathbf{I}}^{j}(\tilde{\mathbf{q}}^{j*})), \tag{39}$$

where $\tilde{I}^{j}(\tilde{q}^{j*}) = \{l_{ik}^{mn}(\tilde{q}^{**}) \forall i = 1, \dots, N_x, k = 1, \dots, N_y, n = 1, \dots, N_t^j, m = 1, \dots, M\}, P_{\tilde{\Lambda}}(x) \text{ is the unique projection of } x \in \tilde{\Lambda} \text{ and is defined as } P_{\tilde{\Lambda}}(x) = Argmin\{||y - x||: y \in \tilde{\Lambda}\}$

Proof. See Appendix B.

With Equation (39), this study adopted the Goldstein-Levitin-Polyak projection algorithm (Goldstein (1964); Levitin and Polyak (1966)) to solve the discretized VI problem. For a given initial travel demand (\tilde{q}_0^j), the subsequent sequence of travel demand (\tilde{q}_w^j) could be generated by the following equation (Equation (40)):

$$\tilde{\boldsymbol{q}}_{w+1}^{j} = P_{\tilde{\Lambda}} \left(\tilde{\boldsymbol{q}}_{w}^{j} - \lambda_{w} \tilde{\boldsymbol{I}}^{j} \left(\tilde{\boldsymbol{q}}_{w}^{j} \right) \right) \tag{40}$$

where λ_w is a given positive step-size of iteration w, which should be set in accordance to the specific problem. To adopt Equation (40), $P_{\tilde{\Lambda}}\left(\tilde{\boldsymbol{q}}_{w}^{j}-\lambda_{w}\tilde{\boldsymbol{I}}^{j}\left(\tilde{\boldsymbol{q}}_{w}^{j}\right)\right)$ should first be known. Based on its definition, $P_{\tilde{\Lambda}}\left(\tilde{\boldsymbol{q}}_{w}^{j}-\lambda_{w}\tilde{\boldsymbol{I}}^{j}\left(\tilde{\boldsymbol{q}}_{w}^{j}\right)\right)$ could be found by solving an equivalent convex quadratic program with the Frank-Wolfe algorithm (Lin et al., 2018).

3.2 Fixed-point formulation for housing location choice problem

To solve for the pollution concentrations (C(x, y, z, t)) that are used in the housing-location choice model, the numerical method for solving the advection-diffusion equation (Equation (27)) with Dirac-type source function (Equation (28) and (29)) should first be established. In this study, the Lax-Friedrichs scheme and standard central finite difference are adopted to approximate the first and second derivatives, respectively, of the advection-diffusion equation. Due to the singularity of the Dirac delta function, the following approximation is adopted (Tornberg and Engquist (2004); ?) (Equation (41)):

$$\delta(z) = \begin{cases} \frac{1}{4\Delta z} \min\left(\frac{z}{\Delta z} + 2, 2 - \frac{z}{\Delta z}\right), & |z| \le 2\Delta z \\ 0, & |z| > 2\Delta z \end{cases}$$
(41)

Here, Δz is the grid size in z direction

For a given $\hat{q}^j = \left\{q_{ik}^{mj} \forall i = 1, \dots, N_x, k = 1, \dots, N_y, m = 1, \dots, M\right\}$, which q_{ik}^{mj} denotes the values of $q^{mj}(x,y)$ at grid point (i,k), PDUO-C model with departure time consideration (Section 2.3) is solved. By Equations (31) \sim (34), $\tilde{\sigma} = \left\{\sigma_{ik} \forall i = 1, \dots, N_x, k = 1, \dots, N_y\right\}$, which σ_{ik} denotes the values of $\sigma(x,y)$ at grid point (i,k), could be found. This could be represented by the following abstract form (Equation (42)):

$$\tilde{\sigma} = \Theta_1 \left(\hat{\mathbf{q}}^j \right) \tag{42}$$

With $\tilde{\sigma}$ in Equation (42), an updated travel demand (\hat{q}^{j}) could be determined by Equation (30) and (35), and could be represented by the following abstract form (Equation (43)):

$$\hat{\mathbf{q}}^j = \Theta_2(\tilde{\boldsymbol{\sigma}}) \tag{43}$$

Considering Equation (42) and (43) the following fixed-point problem could be defined as (Equation 44)):

$$\hat{\mathbf{q}}^{j} = \Theta_{2}\left(\Theta_{1}\left(\hat{\mathbf{q}}^{j}\right)\right) = \Theta_{3}\left(\hat{\mathbf{q}}^{j}\right) \tag{44}$$

3.3 Solution procedure for housing location choice problem

With the fixed-point problems defined in Equation (44), the following solution procedure is adopted to solve the housing location-choice problem.

Step 1. Assume an initial travel demand \hat{q}_w^j based on Q and set w = 1,

Step 2. Solve the PDUO-C model with departure-time consideration

Step 2a Assume an initial travel demand $\tilde{q}_{w_1}^j \in \tilde{\Lambda}$ based on \hat{q}_w^j and set $w_1 = 1$.

Step 2b Compute the travel cost $\phi^m(x, y, t)$ and travel time cost $I^m(x, y, t)$ by solving the PDUO-C model defined in Section 2.1 (see Lin et al. (2018) for details).

Step 2c Compute the schedule delay cost $p^m(x, y, t)$ by using Equation (15).

Step 2d Compute the total travel cost $l^m(x, y, t)$ by using Equation (5).

Step 2e Compute $\tilde{q}_{w_1+1}^j$ by using Equation (40).

Step 2f Compute the relative gap functions. If $\frac{|\tilde{q}_{w_1+1}^j - \tilde{q}_{w_1}^j|}{\tilde{q}_{w_1}^j} \le \varepsilon_1$ and $RGAP_{discrete} \le \varepsilon_2$, go to Step 3; Otherwise set $w_1 = w_1 + 1$ and go to Step 2b.

Step 3. Solve the housing location-choice problem:

Step 3a Set
$$w_2 = 1$$
 and $\hat{q}_{w_2}^j = \hat{q}_w^j$.

Step 3b Compute $\tilde{\sigma}_{w_2}$ by using Equation (31) ~ (34).

Step 3c Compute
$$y_{1,w_2}^j = \Theta_3(\hat{q}_{w_2}^j)$$
 by using $\tilde{\sigma}_{w_2}$ and Equation (44).

Step 3d Compute the step size λ_{w_2} using the method described in Du et al. (2013).

Step 3e Compute
$$\hat{q}_{w_2+1}^j = (1 - \lambda_{w_2})\hat{q}_{w_2}^j + \lambda_{w_2}y_{1,w_2}^j$$

Step 3f If $|\hat{q}_{w_2+1}^j - \hat{q}_{w_2}^j| \le \delta$, go to Step 4; Otherwise set $w_2 = w_2 + 1$ and go to Step 3b.

Step 4. Set
$$y_{2,w}^j = \hat{q}_{w_2+1}^j$$
.

Step 5. Compute the step size λ_w using the method described in Du et al. (2013).

Step 6. Compute
$$\hat{q}_{w+1}^j = (1 - \lambda_w)\hat{q}_w^j + \lambda_w \hat{y}_{2,w}^j$$
.

Step 7. If
$$|\hat{q}_{w+1}^j - \hat{q}_w^j| \le \delta$$
, stop; Otherwise set $w = w + 1$ and go to Step 2.

Noting that $RGAP_{discrete}$ in Step 2f is the discrete form of the relative gap function (Equation (20)) and is defined as follows (Equation (45)):

$$RGAP_{discrete} = \frac{\sum_{m \in \{1, \dots, M\}} \sum_{i \in \{1, \dots, N_x\}} \sum_{k \in \{1, \dots, N_y\}} \sum_{n \in \{1, \dots, N_i\}} q_{ik}^{mn} \left(l_{ik}^{mn} \left(\tilde{\boldsymbol{q}}^{j} \right) - \hat{l}_{ik}^{m} \left(\tilde{\boldsymbol{q}}^{j} \right) \right)}{\sum_{m \in \{1, \dots, M\}} \sum_{i \in \{1, \dots, N_x\}} \sum_{k \in \{1, \dots, N_y\}} q_{ik}^{mj} \hat{l}_{ik}^{m} \left(\tilde{\boldsymbol{q}}^{j} \right)}$$
(45)

4 Numerical experiments

In this section, numerical experiments are set up to demonstrate the proposed models and solution algorithms in the previous sections. In this study, a rectangular modeling region 35

km long and 25 km wide with two CBDs (Figure 3) is adopted as the numerical example. The centers of CBD 1 and 2, respectively, are located at (6 km, 10 km) and (30 km, 15 km). In the modeling region, a $1 \text{ km} \times 1 \text{ km}$ power plant, where traffic is not allowed to enter or leave, is located at (18.5 km, 4.5 km).

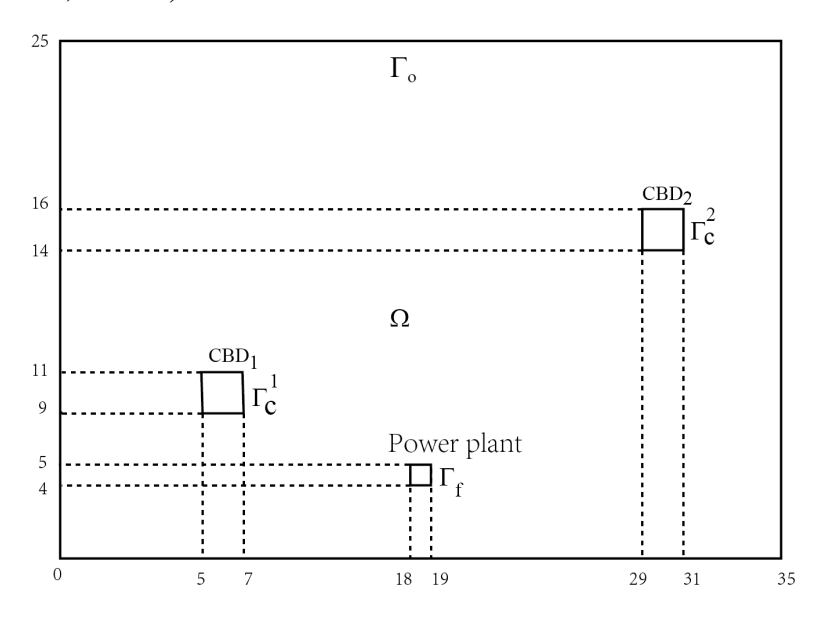


Fig. 3: The rectangular modeling region

In this numerical example, it is assumed that no traffic is present at the beginning of the modeling period (i.e., $\rho_0^m(x,y)=0$, $\forall (x,y)\in\Omega, m\in\{1,\ldots,M\}$) and a zero travel cost at the boundary of CBDs (i.e., $\phi_{CBD}^m=0$, $\forall (x,y)\in\Gamma_c^m, t\in T, m\in\{1,\ldots,M\}$). The modeling period is from 6:00 AM on the first day to 6:00 AM the following day (i.e., $T=[0,24\,h]$), with period 1 from 6:00 AM to 5:00 PM (i.e., $T^1=[0,11\,h]$) and period 2 from 5:00 PM to 6:00 AM in the following day (i.e., $T^2=[11,24\,h]$). It is considered that travelers, regardless of their resident location, will have a similar desired arrival time as they head to, or return from, the CBDs. Thus, the desired arrival times (period 1) and desired departure times (period 2) for this numerical example are defined as: $\{t^{11*}, t^{21*}, t^{12*}, t^{2^*}\} = \{2.8h, 2.3h, 12.5h, 13.0h\}$. For the schedule-delay cost function, the parameters Δ is taken as 0.2 h, whereas γ_1 and γ_2 are taken as 48 \$/h and 108\$/h, respectively. In the speed function, the function $\zeta(x,y)=2\times 10^{-6}km^4/veh^2$, and the free-flow speed of group m travelers is defined as $V_f^m(x,y)=56\left[1+4\times 10^{-3}d(x,y)\right]$, with $d(x,y)=0.75\min\left\{d^1(x,y),d^2(x,y)\right\}+0.25\max\left\{d^1(x,y),d^2(x,y)\right\}$, which $d^1(x,y)$ and

 $d^2(x,y)$ are respective the distance of location (x,y) from the center of CBD 1 and 2. $V_f^m(x,y)$ and d(x,y) are chosen such that the free-flow speed in the domain further from the CBDs is higher due to fewer junctions. In this numerical example, the standard deviation of speed (σ_V^m) and acceleration (σ_a^m) is assumed to be 0.2. For the local travel cost function $(c^m(x,y,t))$, κ is taken as 90\$/h, and $\pi(\rho)$ is taken a functional form of $9 \times 10^{-7} \rho^2$. For the total perceived cost function, θ^1 and θ^2 are taken as 12 and 15, respectively, and the internal operating cost of traffic in CBD 1 and 2, respectively, are defined as $S^1(Q^1) = 8 \times 10^{-11} (Q^1 - 150000)^2$ and $S^2(Q^2) = 10 \times 10^{-11} (Q^2 - 100000)^2$.

In this numerical example, the convergence thresholds are taken as: $\varepsilon_1 = 0.005$, $\varepsilon_2 = 10^{-9}$, and $\delta = 0.01$, it is assumed that the emission rates are: a) $\tilde{\psi}(x,y) = 20(kg/(km^2h))$ within the 1 km × 1 km region of the power plant, and b) $\tilde{\psi}(x,y) = 0.5 \times \frac{L^m(t)}{Q^m}(kg/(km^2h))$ at the m-th CBD with $L^m(t)$ denotes the cumulative number of vehicles in the *m*-th CBD at time *t*. The dispersion of pollutants is modeled within the 1 km space over the rectangular modeling region (i.e., $\hat{\Omega} = [0,35] \times [0,25] \times [0,1]$). It is also assumed that the wind velocity $u_f(x,y,z,t) = (5\sqrt{2},5\sqrt{2},0)$ (in km/h) and eddy diffusivities are both 0.01 km^2/h (i.e., $K_x = K_y = K_z = 0.01$). The fixed total travel demand (Q) is taken as 350,000. Travelers' sensitivity to housing utility in housing location choice ($\hat{\gamma}$) and travelers' sensitivity to perceived cost in destination choice (χ) are respectively taken as 0.0015 and 0.012. The unit cost of pollutant concentration (ξ) is taken as 10 \$km3/kg. These parameters could all be estimated based on the survey results of travelers' choices (e.g., stated preference survey on housing location choice). Details on these estimations are not included as this is not the scope of this study. For housing rent function ($\tau(x,y)$), $\alpha(x,y)$ and $\beta(x,y)$ is respectively taken as 5 and 8. The total housing supply density adopted in $\tau(x,y)$ is defined by:

$$H(x,y) = 1000 \left(1 - \exp\left(-\left(0.5d^{1}(x,y) \right) \right) \right) \left(1 - \exp\left(-\left(0.5d^{2}(x,y) \right) \right) \right)$$
(46)

To verify the convergence of the proposed solution algorithms, three grids (Grid 1: $35 \times 25 \times 50$; Grid 2: $70 \times 50 \times 100$; Grid 3: $140 \times 100 \times 200$) are considered. Figure 4 shows a typical convergence curve of the proposed algorithm under Grid 3: $140 \times 100 \times 200$. Figure 4

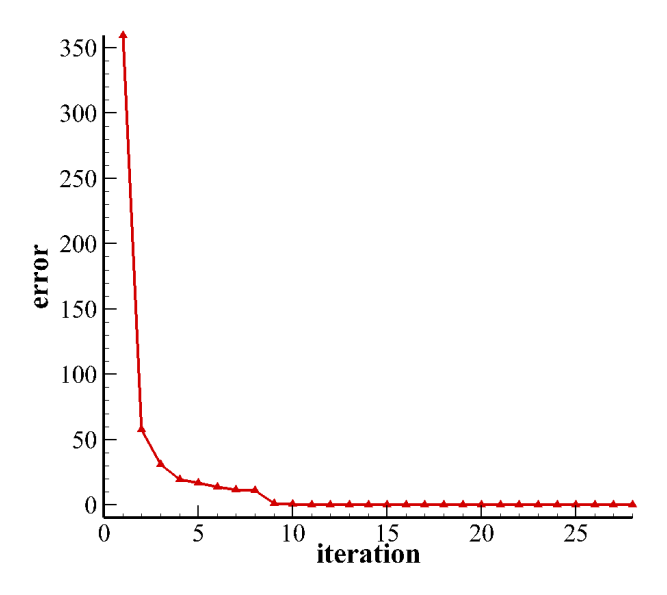


Fig. 4: A typical convergence curve of the proposed solution algorithm.

also shows that the error $(|\hat{q}_{w+1}^{j} - \hat{q}_{w}^{j}|)$ substantially deceases in the first few iterations, whereas such a decrease becomes extremely small after the 12-th iteration. In general, the proposed algorithm converges in solving the housing-location problem proposed in this study. Figure 5, which shows the variation in demand in various locations of x and y, are typical examples of the grid convergence of different discretization schemes (i.e., Grids 1–3). Compare to the other two grids, Grid 3 (140 × 100 × 200) shows good convergence in numerical solution and is thus adopted in the remainder of this numerical example.

Figure 6 shows the temporal variation in travel demand and the total travel cost (6:00 AM–12:00 PM) for each group of travelers at different points within the modeling region. A comparison of the peak demand for each group of travelers with the corresponding total travel cost shows that the peak is always located at the time when the total travel cost reaches its minimum. It could be concluded that all travelers will choose a departure time such that the total travel costs are equal and minimized, and thus the simultaneous dynamic user-optimal and departure-time principle will be satisfied. As the desired arrival time of the group 1 travelers (2.8 h) is later than that of the group 2 travelers (2.3 h), their departure times (i.e., the time having the peak) are always later than those of the group 2 travelers. Each subfigure of

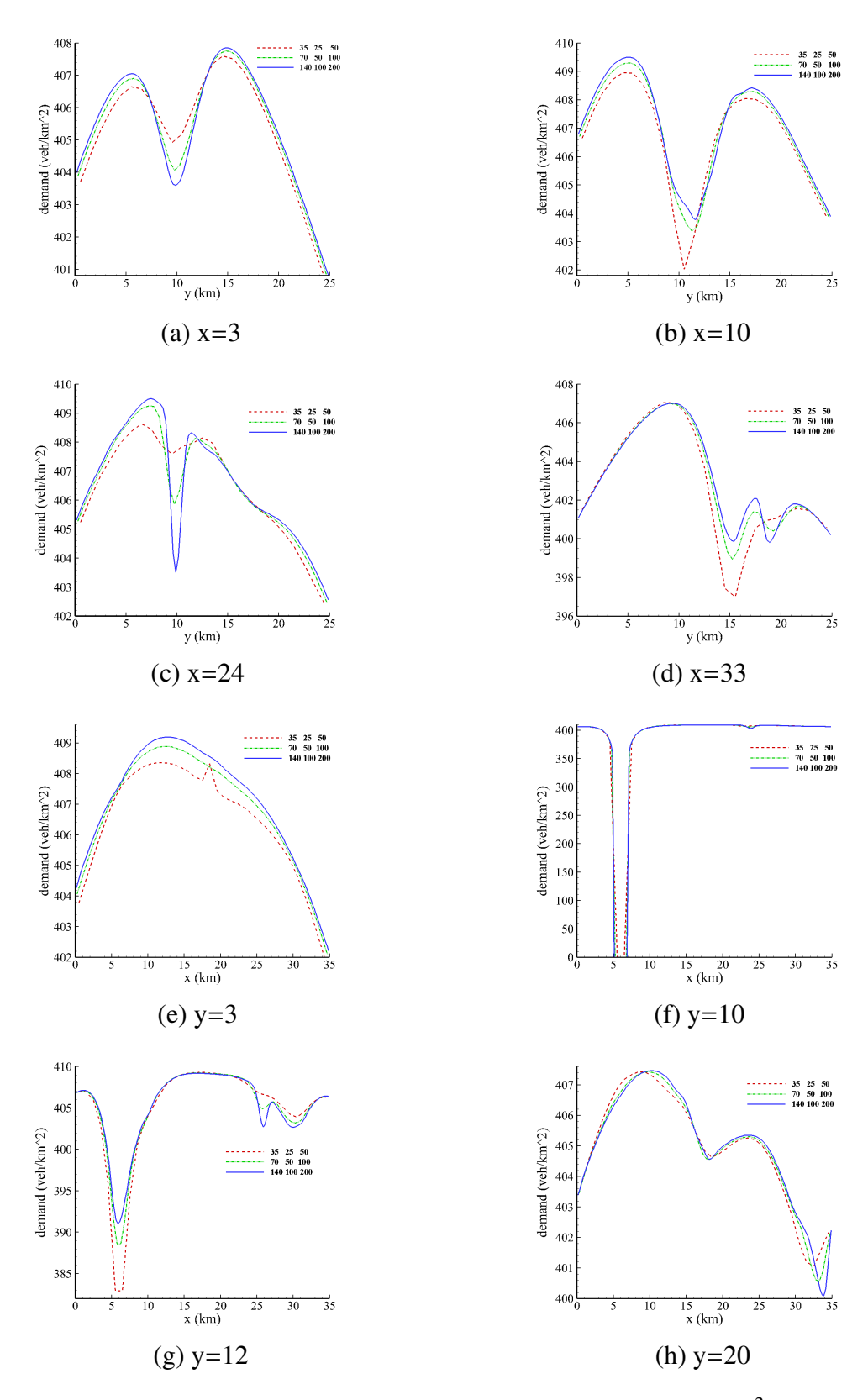


Fig. 5: The grid convergence of the demand. (unit: veh/km^2).

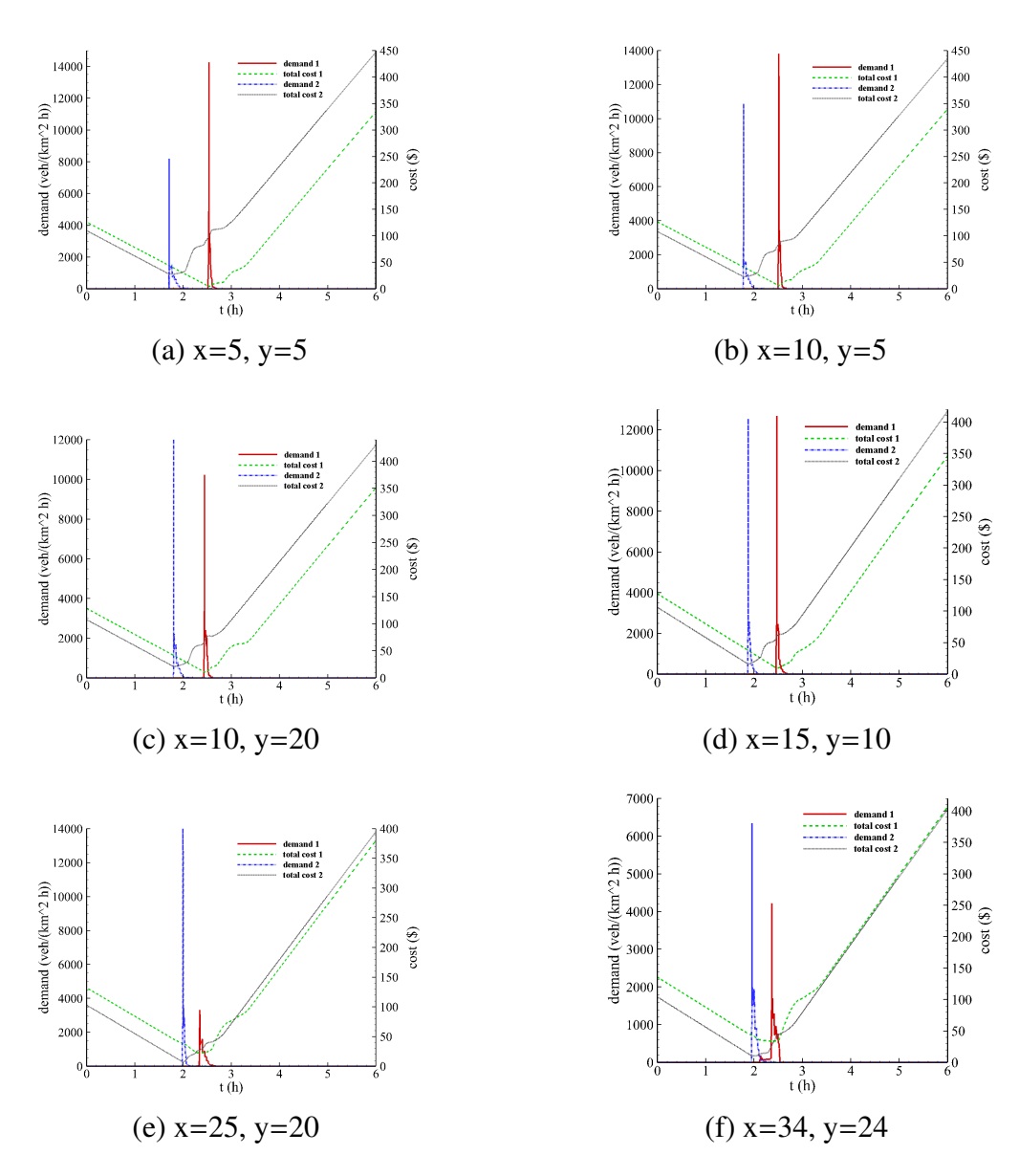


Fig. 6: The travel demand and total travel cost for traveling to the CBD (j = 1).

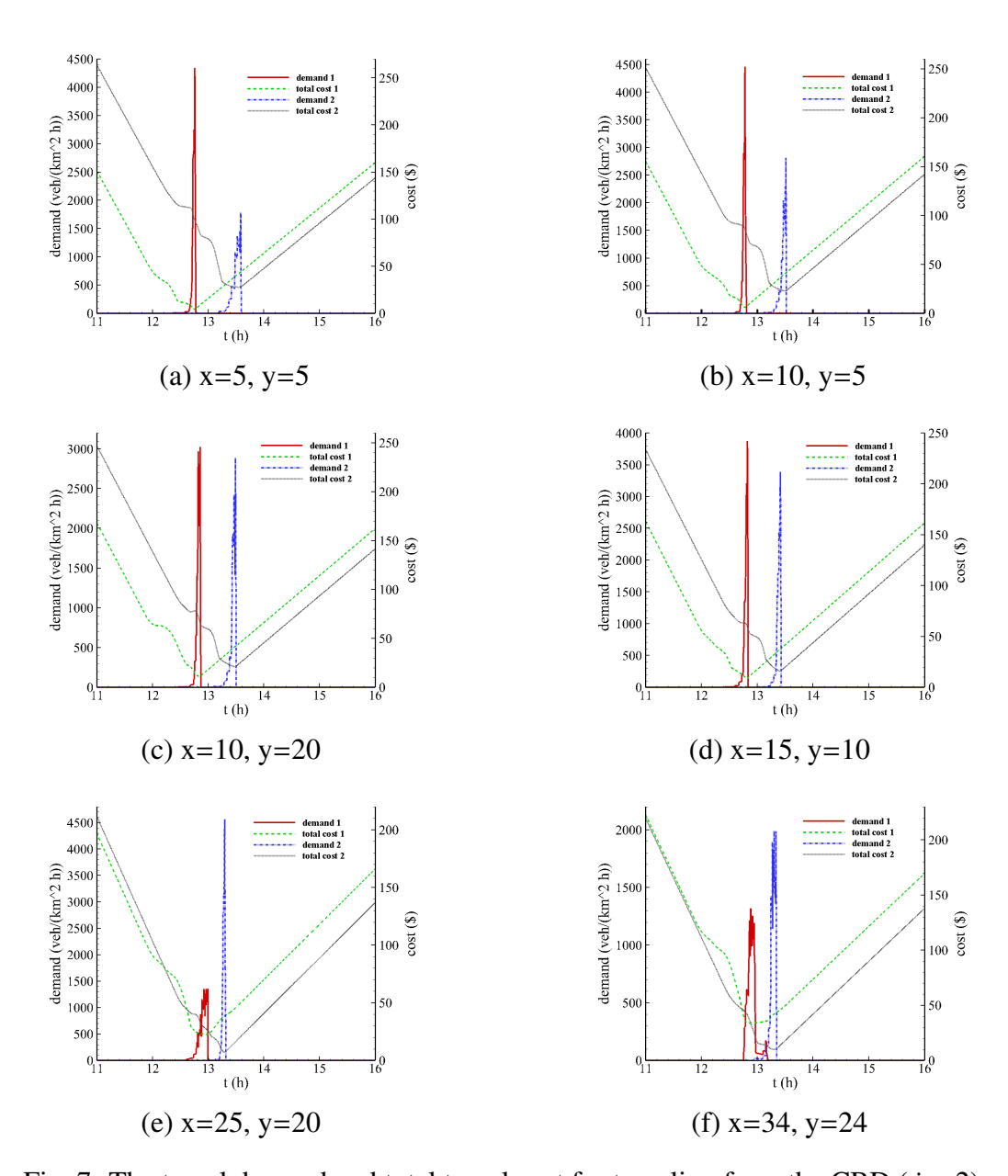


Fig. 7: The travel demand and total travel cost for traveling from the CBD (j = 2).

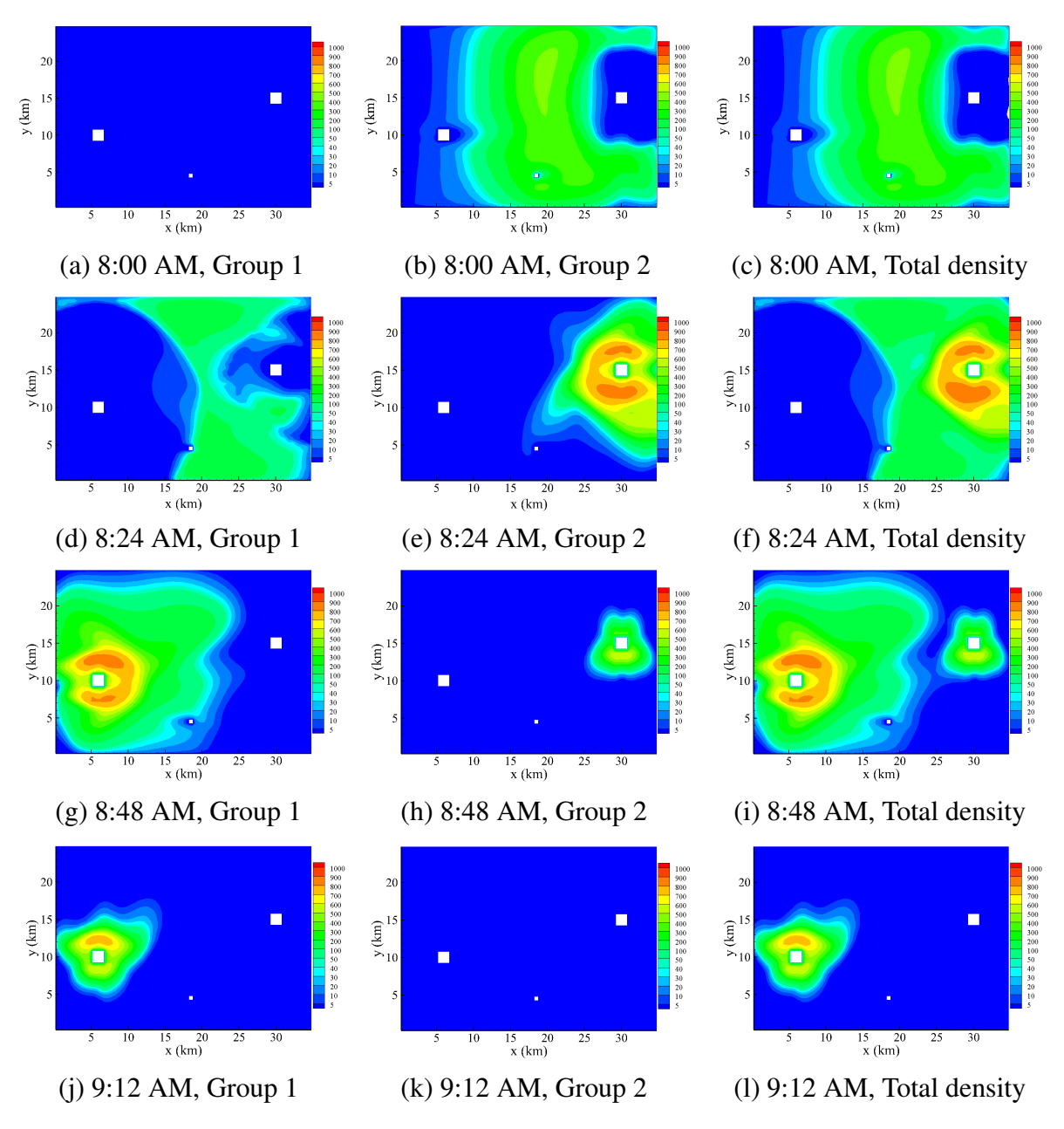


Fig. 8: The density plots for travelers traveling to CBDs (unit: veh/km^2).

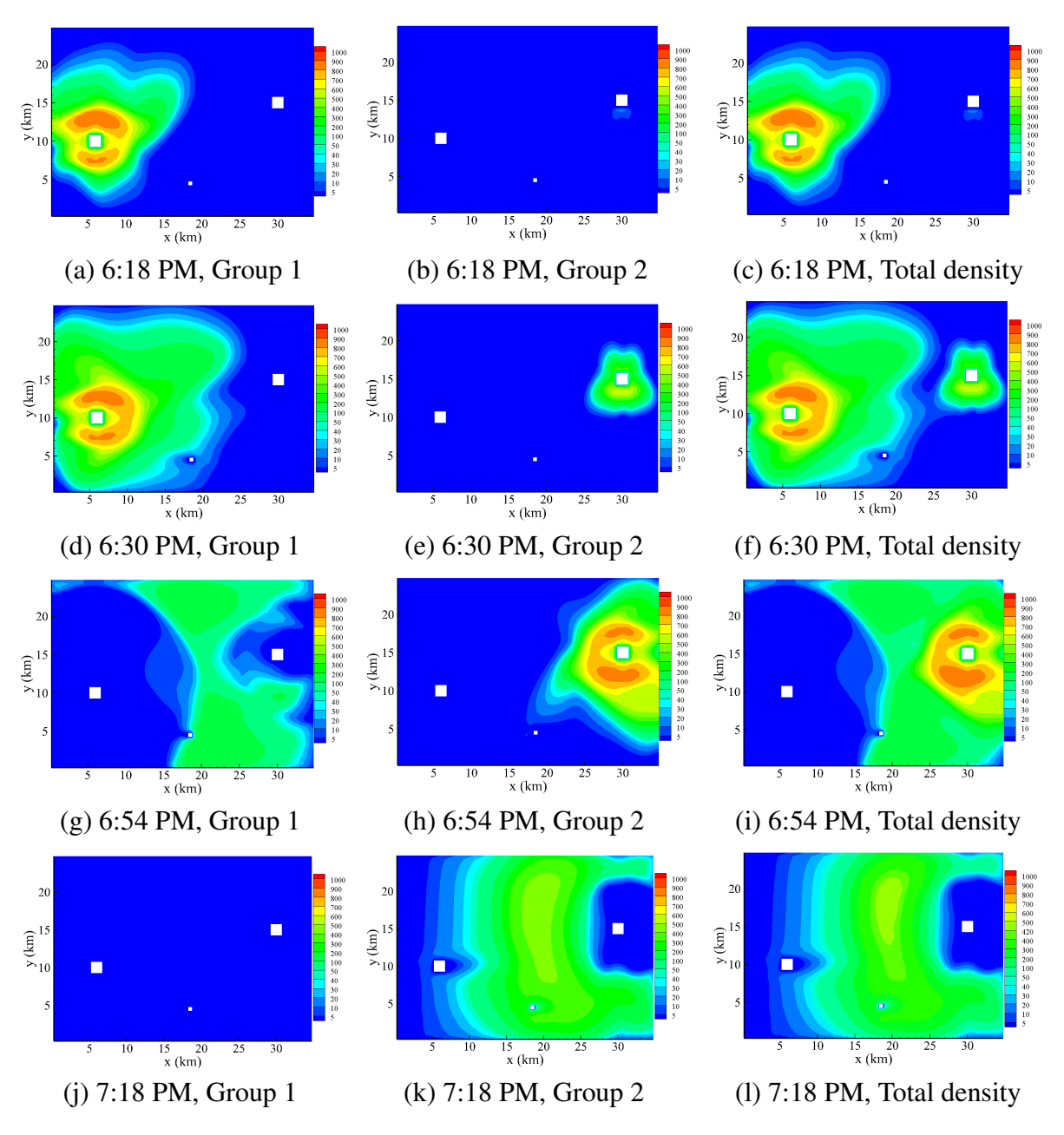


Fig. 9: The density plots for travelers returning from CBDs (unit: veh/km^2).

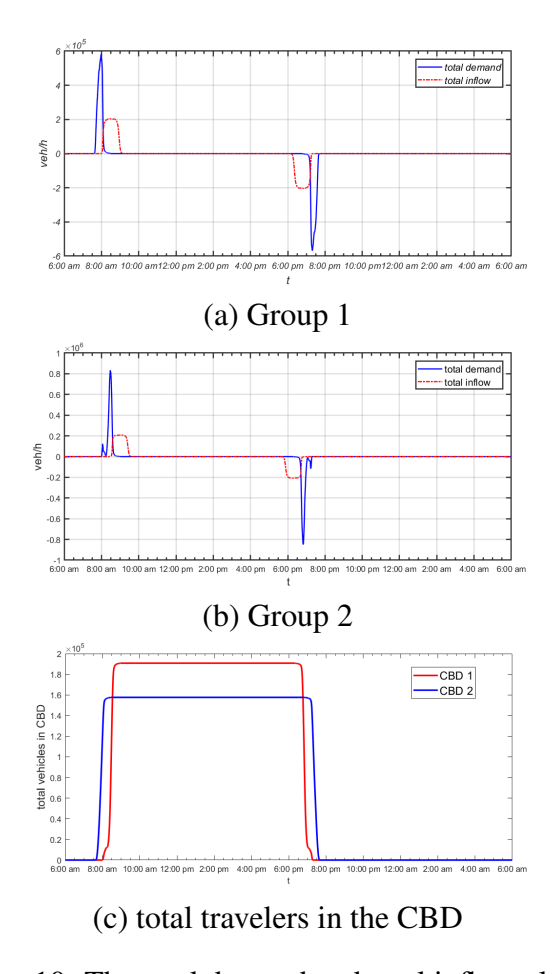


Fig. 10: The total demand and total inflow plot.

Figure 6 shows that in the beginning (ending) period, the total travel cost ($l^m(x, y, t)$) decreases (increases) at a constant rate of 48 \$/h (108 \$/h) because in the beginning (ending) period, the modeling region is uncongested and, thus, the actual travel cost ($\phi^m(x, y, t)$) should be relatively constant in this period. Therefore, the changes in the total travel cost are affected only by the schedule-delay cost (i.e., the early- and late-arrival penalties) that has a linear relationship with the departure time with respect to the value of time for early or late arrival ($\gamma_1 = 48$ \$/h and $\gamma_2 = 108$ \$/h).

Figure 7 shows the temporal variation in travel demand and the total cost (5:00 PM–12:00 AM) for each group of travelers traveling from the CBDs to various locations (i.e., their own housing location) within the modeling region. Similar to the period during which the travelers are traveling to the CBDs (Figure 6), the dynamic user-optimal and departure-time principles

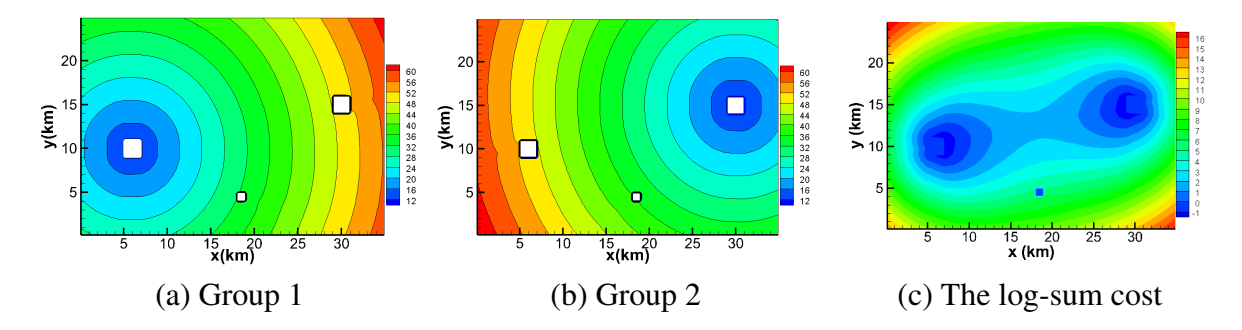


Fig. 11: Total perceived travel costs to CBDs in modeling period 1.

are also satisfied. As the desired departure time of the group 2 travelers (13.0 h) is later than that of the group 1 travelers (12.5 h), their departure times (i.e., the time with the peak demand) are always later than those of the group 2 travelers. Each subfigure of Figure 7 shows that in the beginning (ending) period, the total travel cost ($l^m(x, y, t)$) decreases (increases) at a constant rate of 108 \$/h (48 \$/h) because the modeling region is uncongested during the period, and thus the actual travel cost should be relatively constant in this period. Therefore, the changes in the total travel cost are affected only by the schedule-delay cost (i.e., the early- and late-arrival penalties), which has a linear relationship with the departure time with respect to the value of time for early or late departure ($\gamma_1 = 48$ \$/h and $\gamma_2 = 108$ \$/h).

Figure 8 shows the temporal and spatial distribution of density ($\rho^m(x, y, t)$) for the two groups of travelers within the modeling region as they travel to the CBDs in modeling period 1 (j = 1). Figure 8a, 8b, and 8c shows that most travelers are from group 2 and are traveling to CBD 2 (i.e., the CBD on the right). The density of group 2 travelers around CBD 2 is lower because: 1) the travelers who reside further away and have departed have not yet arrived in this area; and 2) the travelers who reside in this area have not yet departed due to their shorter required travel time. At 8:00 AM, there are very few group 1 travelers (Figure 8a) because this group of travelers has a desired arrival period of 8:48 AM–9:12 AM; thus, they will not depart at this time (or earlier) to avoid the early-arrival penalty. At 8:24 AM, the group 1 travelers begin to depart for their destination (Figure 8d) while the group 2 travelers, who have a desired

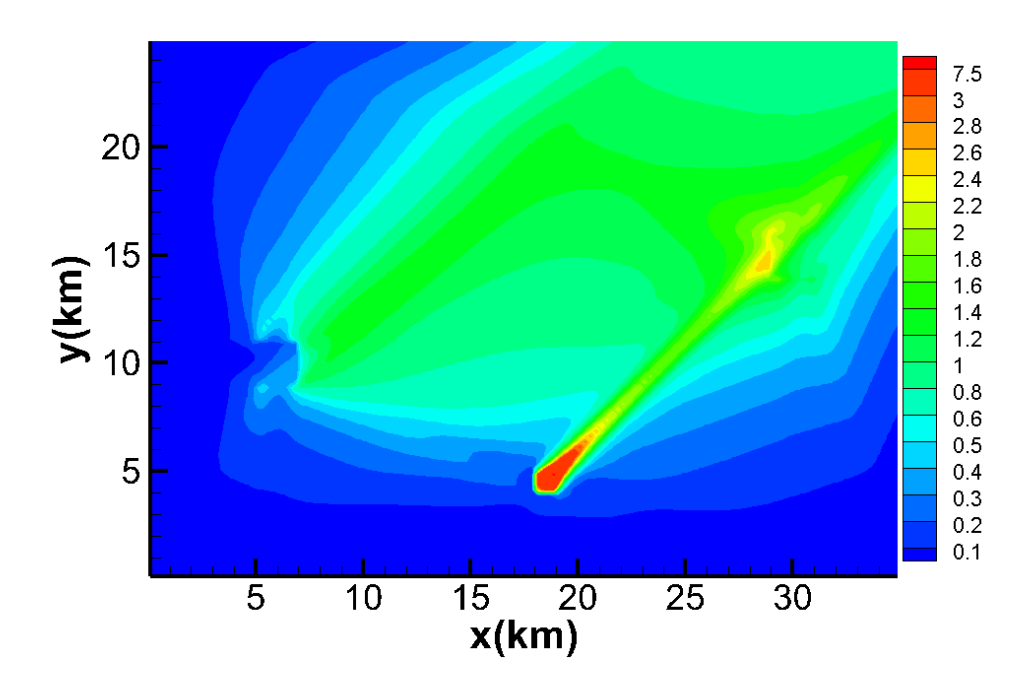


Fig. 12: Average pollutant concentrations (unit: kg/km^3).

arrival period of 8:36 AM–9:00 AM, have nearly reached their destination, resulting in a high density of this type of traveler in the vicinity of CBD 2 (Figure 8e). At 8:48 AM, the group 1 travelers have nearly reached their destination, resulting in a high density of this type of traveler in the vicinity of CBD 1 (Figure 8g). The density of group 2 travelers is lower at 8:48 AM (Figure 8h) than at 8:24 AM (Figure 8e) because they have arrived at their destination and have left the transportation system. At 9:12 AM, all group 2 travelers have left the system, but some group 1 travelers remain (Figure 8j and Figure 8k).

Figure 9 shows the temporal and spatial distributions of density ($\rho^m(x, y, t)$) for the two groups of travelers within the modeling region as they return from the CBDs. Figure 9(a), 9(b), and 9(c) shows that most travelers from group 1 are returning from CBD 1 (i.e., the CBD on the left). The density of group 1 travelers is relatively high in the vicinity of CBD 1 because these travelers, who reside further away from CBD 1, have just departed and have not yet arrived at their housing location. At 6:18 PM, very few group 2 travelers remain (Figure 9(b)) because this group of travelers has a desired departure period of 6:48 PM–7:12 PM, so they will not depart at this time (or earlier) to avoid the early-departure penalty. At 6:30 PM,

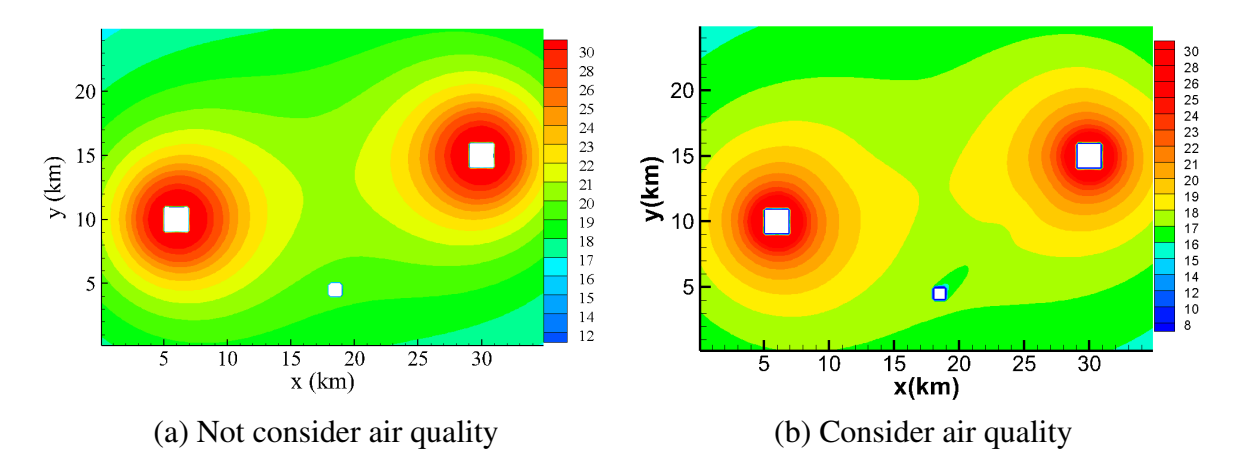


Fig. 13: Housing rent (unit: \$).

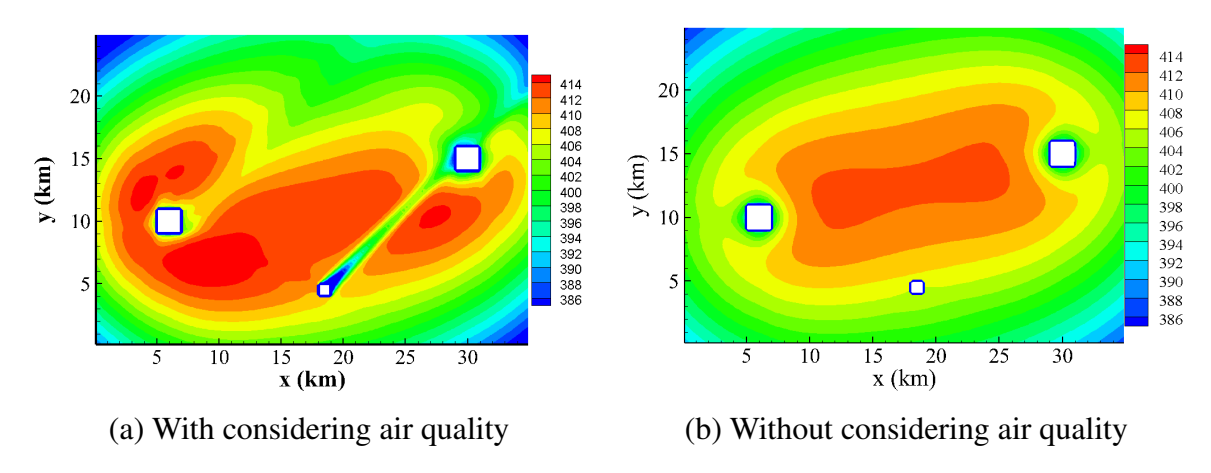


Fig. 14: Total travel demand plot (unit: veh/km^2).

the group 2 travelers start to depart CBD 2 (Figure 9(e)), whereas the group 1 travelers, who have a desired arrival period of 6:18 PM–6:42 PM, have nearly departed CBD 1, resulting in a high density of this type of traveler in the vicinity of CBD 1 (Figure 9(d)). At 6:54 PM, the group 2 travelers have nearly departed CBD 2, resulting in a high density of this type of traveler in the vicinity of CBD 2 (Figure 9(h)). The density of group 1 travelers at 6:54 PM (Figure 9(g)) is lower than at 6:30 PM (Figure 9(d)) because they have reached their destinations and left the transportation system. At 7:18 PM, all group 1 travelers have left the system, and some group 2 travelers remain (Figure 9(j) and Figure 9(k)).

Figure 10 shows the temporal relationship between the inflows of CBDs and the corresponding demand within the modeling region. Noted that the inflows of CBDs ($F_{CBD}^m(t)$) and the corresponding total demand within the modeling region ($Q_{\Omega}^m(t)$) are defined by the following equations:

$$F_{CBD}^{m}(t) = \int_{\Gamma_{c}^{n}} \mathbf{f}^{m}(x, y, t) \cdot \tilde{\mathbf{n}}(x, y) d\Gamma, \quad \forall m \in \{1, \dots, M\}, t \in T$$
 (47)

$$Q_{\Omega}^{m}(t) = \iint_{\Omega} q^{m}(x, y, t) d\Omega, \quad \forall m \in \{1, \dots, M\}, t \in T$$
(48)

where \tilde{n} is the unit normal vector pointing toward the CBD that gives $f^m(x,y,t) \cdot \tilde{n}(x,y)$ is larger (smaller) than zero to represent the inflow (outflow). Numerical integration shows that the area under these two curves (i.e., red and blue) in modeling period 1 (also period 2) are the same for each group of travelers (Figure 10 (a) and 10(b)). Taking the group 1 travelers in modeling period 1 as an example, this indicates that all travelers have arrived at the CBD by 9:00 AM (i.e., the time the inflow curve drops to zero). In modeling period 1 (i.e., 6:00 AM–5:00 PM), the curves for total inflow ($F^m_{CBD}(t)$) always lag behind the total demand ($Q^m_{\Omega}(t)$) because it takes time for the travelers to travel to the CBD (Figure 10 (a) and 10(b)). This sequence is reversed in modeling period 2 as travelers flow out of the CBDs and back to their homes. The number of travelers/vehicles in the modeling region increases (decreases) when the cumulative total demand is greater (less) than the cumulative inflow. Figure 10(c) shows the temporal distribution of travelers/vehicles in CBDs and indicates that all group 1 (group

2) travelers/vehicles remained in CBD 1 from 9:00 AM to 6:00 PM (CBD 2 from 8:30 AM to 6:30 PM), which makes the emission rate within the CBD the highest in this period.

Figure 11 shows the total perceived travel cost for various groups of travelers and the overall log-sum costs. Figure 11(a) and 11(b) shows that the total perceived travel cost increases with the distance to the destination. For the log-sum cost (Figure 11(c)), it can be seen that the area between CBD 1 and 2 has the lowest value, which indicates that this area is a relatively convenient housing (home) location for those who travel to both CBDs. Figure 12 shows the spatial distribution of the average air pollutant (NO_x) concentration at ground level ($\bar{C}(x, y, 0)$)). This figure shows that the downwind locations (i.e., the upper-right corner of the modeling region) are much more polluted than the upwind locations. In particular, the severe emissions from the power plant make the corresponding downwind locations the most polluted area. In addition to this area, the vicinity around CBD 2 is also highly polluted because it is downwind from the modeling region and the high intensity of traffic flow. The vicinity around CBD 1 is less polluted than the area around CBD 2 because the emitted pollutants are dispersed by the wind to the northeast. Figure 13 shows the spatial distribution of housing rent (r(x, y)) with and without considering the air quality. Comparing these two figures, it could be seen that the housing rent is extremely high near the CBDs, which could be explained by the limited housing provision (H(x, y)) and high demand (q(x, y)) in these areas. For the downwind locations of the power plant, the housing rent is relatively lower than in the surrounding areas, which can be explained by the fact that the high concentration of pollutants in this area (Figure 12) lowers its attractiveness (Equation 30) and, thus, reduces the housing rent.

Figure 14 shows the spatial distribution of total travel demand within the modeling region (q(x,y)) with (Figure 14(a)) and without (Figure 14(b)) considering air quality in the housing location choice (Equation 29 and 30). Both figures show that the travel demands attain a maximum at a certain distance from the CBDs (i.e., the demand decreases as it gets closer to the CBDs), which could be explained by the travelers' trade-off in choosing their housing location. For Figure 14(a), this trade-off is between travel cost, housing rent and air quality,

while it is between travel cost and housing rent for Figure 14(b). From figure 14(a), moving from the outer boundary of the modeling region to the CBDs, the housing utility $(\sigma(x, y))$ increases because the decrease in the log-sum of the perceived travel cost $(\Pi(x, y))$ outweighs the increase in housing rent (r(x, y)) and the lower air quality ($\tau(x, y)$). Thus, as the housing utility increases, the demand increases nearer the CBDs. As it moves toward the CBDs, housing rent will continuously increase (due to the limited housing provision) and air quality will continue to worsen (due to the more congested traffic), while the travel costs are reduced due to the shorter distance to travel. Thus, it will come to a point where the decrease in travel costs can no longer cover the increase in housing rent and worsening of air quality. Beyond this point, the housing utility and thus also the housing demand will decrease. Compared Figure 14(a) and 14(b), it could be seen that, in general, travel demands are more concentrated in the south-western region (upwind region) for the case of considering air quality in housing location choice model (Figure 14(a)) than that air quality is not considered (Figure 14(b)). This could be explained by the fact that air pollutants are less concentrated at the upwind location due to the dispersion along the wind direction (i.e., towards northeast). Such observation also exists in the upwind (south-western) and downwind (north-eastern) region around the CBDs (especially CBD 1) and the power plant (comparing Figure 14(a) and 14(b)). Despite the travel demand pattern is similar in these regions, the major source of air pollutants for these regions are different. For the region around power plant, the major source of air pollutants is from the power plant, while for the region around CBD, the major source is from traffic emission due to the high congestion in these areas (Figure 8 and 9).

To measure the residents' health risk, the following health cost (Υ) is defined based on the distribution of demand and pollution concentration:

$$\Upsilon = \iint_{\Omega} \bar{C}(x, y, 0) q(x, y) d\Omega \tag{49}$$

Table 1: Health risk Υ under three free-flow speeds.

$V_f^m(\text{km/h})$	Total travel time (h)	Total emission (kg/km)	Υ
46	1203	304	125697
56	1156	313	129244
66	1087	319	136872

Table 1 shows the health risk (Υ) and other related quantities (total travel time and total emission) for three free-flow speeds (V_f^m). Table 1 shows that when the free-flow speed increases the total travel time—or the total duration that pollutants are emitted—is decreased as expected. In contrast, based on Equation (21) and (23), the emission rate increases as the free-flow speed, or the speed of the vehicles, increases. As the reduction in the emission duration (total travel time) cannot cover the increase in emission rate, the total emissions increase as the free-flow speed increases (column 3 of Table 1). Finally, owing to the fixed demand of the numerical example (i.e., 350,000), the increase in total emissions will cause an increase in health risk.

5 Conclusions

In this study, a predictive continuum dynamic user-optimal model (PDUO-C) is presented with combined housing location, destination, route, and departure-time choice in a polycentric city. Travelers' choice of housing location is modeled by a logit-type demand distribution function with air quality, housing rent, and perceived travel cost as the selection criteria. In this study, air quality is quantified by the concentration of air pollutants from vehicle exhaust and other point sources (e.g., power plants). Vehicle exhaust is modeled with the vehicle emission model, which depends on instantaneous acceleration and speed, and is dispersed based on the three-dimension advection-diffusion equation, which depends on the turbulent eddy motion and wind. PDUO-C with simultaneous route and departure-time choice is adopted to evaluate the perceived travel cost to determine the destination and housing location choice.

The housing-location problem is formulated as a fixed-point problem, and the PDUO-C

model with departure-time consideration is formulated as a VI problem. The Lax-Friedrichs scheme is adopted to discretize/solve the conservation law, Hamilton-Jacobi equation and advection-diffusion equation, and the fast-sweeping method is adopted to solve the Eikonal equation. The Goldstein-Levitin-Polyak projection algorithm and self-adaptive successive averages are adopted to solve the proposed fixed-point and VI problem. A numerical example is given to demonstrate the characteristics of the proposed housing-location choice problem with consideration of air quality and the effectiveness of the solution algorithms. In this study, it is found that the housing location pattern (i.e., the demand location) could be substantially changed if air quality is considered in the housing location choice model. Such consideration of air quality will help to provide a more realistic and comprehensive modeling of housing location choices that will directly affects the travel and congestion patterns. This will then help to precisely model the responses – in housing location, destination, and route choice – of citizens/travelers in the evaluation and design of various land-use and transport plans (e.g., housing policy).

Acknowledgements

The study described in this paper was supported by a grant from the Research Grants Council of the Hong Kong Special Administrative Region, China (Project No. 17208614). The second author was also supported by the Francis S Y Bong Professorship in Engineering. The research of the third author is supported by NSFC Grant 11471305, and the research of the fourth author was supported by NSF grant DMS-1719410.

Appendix A Detailed proof of Theorem 1

Theorem A.1. The dynamic user-optimal condition in Definition 1 is equivalent to the following variational inequality problem in modeling period j: Find $\mathbf{q}^{j^*} \in \Lambda^j$ so that for all $\mathbf{q}^j \in \Lambda^j$

(Equation (A.1)),

$$\sum_{m \in \{1, M\}} \iint_{\Omega} \int_{T^j} l^m \left(x, y, t, q^{j^*} \right) \left(q^m (x, y, t) - q^{m^*} (x, y, t) \right) dt d\Omega \ge 0 \tag{A.1}$$

Proof. (Necessity) Suppose that $q^j \in \Lambda^j$ is any feasible travel demand and $q^{j^*} \in \Lambda^j$ is the travel demand that satisfies the dynamic user-optimal condition (Equation (17)). For some location $(x, y) \in \Omega$ and time $t \in T^j$ such that $q^m(x, y, t) - q^{m^*}(x, y, t) < 0$, Equation (17) could be used to prove that (Equation (A.2)):

$$0 \le q^{m}(x, y, t) < q^{m^{*}}(x, y, t)$$

$$\Rightarrow l^{m}(x, y, t, q^{j^{*}}) - \hat{l}^{mj}(x, y, t, q^{j^{*}}) = 0.$$
(A.2)

With Equation (A.2) and the fact that $l^m(x, y, t, \mathbf{q}^{j^*}) - \hat{l}^{mj}(x, y, \mathbf{q}^{j^*}) \ge 0$ from Equation (17), the following equation is satisfied (Equation (A.3)):

$$(l^{m}(x, y, t, \mathbf{q}^{j^{*}}) - \hat{l}^{mj}(x, y, \mathbf{q}^{j^{*}})) (q^{m}(x, y, t) - q^{m^{*}}(x, y, t)) \ge 0,$$
(A.3)

Integrating Equation (A.3) over space and time, and summing up for all groups of travelers, it could be shown that (Equation (A.4)):

$$\sum_{m \in \Omega} \iint_{\Omega} \int_{T^{j}} \left(l^{m}\left(x, y, t, \boldsymbol{q}^{j^{*}}\right) - \hat{l}^{mj}\left(x, y, \boldsymbol{q}^{j^{*}}\right) \right) \left(q^{m}(x, y, t) - q^{m^{*}}(x, y, t) \right) dt d\Omega \ge 0, \quad (A.4)$$

From Equation (A.4), because $\hat{l}^{mj}(x,y,q^{j^*})$ is independent of time and from the definition of $q^m(x,y,t)$ that $\int_{T^j} (q^m(x,y,t)-q^{m*}(x,y,t)) dt = 0$, Equation (A.1) follows.

(sufficiency) Suppose that $q^{j^*} \in \Lambda^j$ satisfies Equation (A.1) for all $q^j \in \Lambda^j$. Based on the definition of $\hat{l}^{mj}(x,y,q^j)$ in Equation (16), it could be shown that (Equation (A.5)):

$$l^{m}\left(x, y, t, \boldsymbol{q}^{j^{*}}\right) \ge \hat{l}^{mj}\left(x, y, \boldsymbol{q}^{j^{*}}\right),\tag{A.5}$$

Thus, based on the above equation, q^{j*} satisfies the $q^m(x,y,t)=0$ case of Equation (17). For the case $q^m(x,y,t)>0$, the proof will be completed by contradiction. Assume that the $q^m(x,y,t)>0$ case of Equation (17) is not satisfied for traveller; s group m_a at location $(x_a,y_a)\in\Omega$ at time $t_a\in T^j$, such that (Equation (A.6)):

$$q^{m_a^*}(x_a, y_a, t_a) > 0, \quad l^{m_a}(x_a, y_a, t_a, \mathbf{q}^{j^*}) - \hat{l}^{m_a j}(x_a, y_a, \mathbf{q}^{j^*}) > 0, \tag{A.6}$$

With the continuity of $q^{m_a^*}(x, y, t)$, $l^{m_a}(x, y, t, q^{j^*})$ and $\hat{l}^{m_a, j}(x, y, q^{j^*})$, there exist positive values $\delta > 0$, $\varepsilon > 0$ and a neighbor $(\Omega_a \times T_a^j)$ around (x_a, y_a, t_a) such that (Equation (A.7)):

$$q^{m_a^*}(x,y,t) > \delta, \quad l^{m_a}\left(x,y,t,\boldsymbol{q}^{j^*}\right) - \hat{l}^{m_a,j}\left(x,y,\boldsymbol{q}^{j^*}\right) > 2\varepsilon, \quad \forall (x,y) \in \Omega_a, t \in T_a^j, \tag{A.7}$$

Note that the set Ω_a and T_a^j has a positive measure (i.e., $|\Omega_a| > 0$ and $|T_a^j| > 0$). Then according to the definition of $\hat{l}^{m_a,j}\left(x,y,q^{j^*}\right)$, there exist positive values $\varepsilon_1>0$ and a non-empty set $T_b^j\subset T^j$, such that(Equation (A.8)):

$$l^{m_a}\left(x_a, y_a, t, \boldsymbol{q}^{j^*}\right) < \hat{l}^{m_a j}\left(x_a, y_a, \boldsymbol{q}^{j^*}\right) + \varepsilon_1, \quad \forall t \in T_b^j$$
(A.8)

Again, with the continuity of $l^{m_a}(x, y, t, \mathbf{q}^{j^*})$ and $\hat{l}^{m_a j}(x, y, \mathbf{q}^{j^*})$, there exist positive value $\varepsilon' > 0$ and a neighbor $(\Omega_b \times T_b^j)$ around (x_a, y_a, t_a) such that (Equation (A.9)):

$$l^{m_a}\left(x, y, t, \boldsymbol{q}^{j^*}\right) - \hat{l}^{m_a j}\left(x, y, \boldsymbol{q}^{j^*}\right) < \varepsilon', \forall (x, y) \in \Omega_b, t \in T_b^j, \tag{A.9}$$

Note that the set Ω_b and T_b^j has a positive measure (i.e., $|\Omega_b| > 0$ and $|T_b^j| > 0$). Without loss of generality, it could be assumed that $\Omega_a = \Omega_b$, $T_a^j \cap T_b^j = \emptyset$, $|T_a^j| = |T_b^j|$ and $\varepsilon = \varepsilon'$. Then, a $q^j \in \Lambda^j$ that contradicts the case of Equation (17) is constructed as follows (Equation (A.10)):

$$q^{m}(x, y, t) = \begin{cases} q^{m^{*}}(x, y, t) - \delta, \forall (x, y) \in \Omega_{a}, t \in T_{a}^{j}, m = m_{a} \\ q^{m^{*}}(x, y, t) + \delta, \forall (x, y) \in \Omega_{a}, t \in T_{b}^{j}, m = m_{a} \\ q^{m^{*}}(x, y, t), \text{ otherwise} \end{cases}$$
(A.10)

If $m=m_a$, $(x,y)\in\Omega_a$ and $t\in T_a^j$, by Equation (A.7) and Equation (A.9), it could be shown that:

$$q^{m^*}(x, y, t) > \delta \Rightarrow q^m(x, y, t) = q^{m^*}(x, y, t) - \delta > 0,$$
 (A.11)

If $m = m_a$, $(x, y) \in \Omega_b$ and $t \in T_b^j$, by Equation (A.6) and Equation (A.9), it could be shown that:

$$q^{m^*}(x, y, t) > 0 \Rightarrow q^m(x, y, t) = q^{m^*}(x, y, t) + \delta > 0,$$
(A.12)

otherwise by Equation (A.9),

$$q^{m}(x, y, t) = q^{m^{*}}(x, y, t) > 0$$
(A.13)

Moreover, for $m = m_a$

$$\int_{T^{j}} q^{m}(x, y, t) dt = \int_{T^{j} \setminus T_{a}^{j} \setminus T_{b}^{j}} q^{m}(x, y, t) dt + \int_{T_{a}^{j}} q^{m}(x, y, t) dt + \int_{T_{b}^{j}} q^{m}(x, y, t) dt
= \int_{T^{j} \setminus T_{a}^{j} \setminus T_{b}^{j}} q^{m^{*}}(x, y, t) dt + \int_{T_{a}^{j}} \left[q^{m^{*}}(x, y, t) - \delta \right] dt + \int_{T_{\delta}^{j}} \left[q^{m^{*}}(x, y, t) + \delta \right] dt
= q^{mj}(x, y)$$
(A.14)

Thus, $q^m(x, y, t)$ constructed in Equation (A.10) is within the feasible set Λ^j . Then, with the constructed $q^m(x, y, t)$ in Equation (A.10), consider:

$$\sum_{1 \leq m \leq M} \iint_{\Omega} \int_{T_{a}^{j}} l^{m}(x, y, t, q^{j^{*}}) (q^{m}(x, y, t) - q^{m^{*}}(x, y, t)) dt d\Omega$$

$$= \iint_{\Omega_{a}} \int_{T_{a}^{j} \cup T_{b}^{j}} l^{m_{a}}(x, y, t, q^{j^{*}}) (q^{m_{a}}(x, y, t) - q^{m^{*}}(x, y, t)) dt d\Omega$$

$$= \iint_{\Omega_{a}} \left[\int_{T_{a}^{j}} -\delta l^{m_{a}}(x, y, t, q^{j^{*}}) dt + \int_{T_{b}^{j}} \delta l^{m_{a}}(x, y, t, q^{j^{*}}) dt \right] d\Omega$$

$$\leq \iint_{\Omega_{a}} \left[\int_{T_{a}^{j}} -\delta (\hat{l}^{m_{a}j}(x, y, q^{j^{*}}) + 2\varepsilon)) dt + \int_{T_{b}^{j}} \delta (\hat{l}^{m_{a}j}(x, y, q^{j^{*}}) + \varepsilon)) dt \right] d\Omega$$

$$= \iint_{\Omega_{a}} (-\delta |T_{a}^{j}| (\hat{l}^{m_{a}j}(x, y, q^{j^{*}}) + 2\varepsilon)) + \delta |T_{b}^{j}| (\hat{l}^{m_{a}j}(x, y, q^{j^{*}}) + \varepsilon)) d\Omega$$

$$= \iint_{\Omega_{a}} (-\delta |T_{a}^{j}| \varepsilon) d\Omega$$

$$= -\delta |T_{a}^{j}| \Omega_{a}| \varepsilon < 0 \tag{A.15}$$

This contradicts Equation (A.1) for this choice of $q^j \in \Lambda^j$, and the $q^m(x, y, t) > 0$ case of Equation (17) is thus proved by contradiction. Thus, $q^{j^*} \in \Lambda j$ that satisfies the variational inequalities problem (Equation (A.1) or Equation (18)), is equivalent to the satisfaction of the dynamic user-optimal condition with departure-time consideration defined in Equation (17).

Appendix B Detailed proof of Theorem 2

Theorem B.1. Let $\lambda > 0$, \tilde{q}^{j^*} is a solution of the variational inequality problem (equation 35) if and only if (Equation (B.1)):

$$\tilde{\boldsymbol{q}}^{j^*} = P_{\tilde{\Lambda}}(\tilde{\boldsymbol{q}}^{j^*} - \lambda \tilde{\boldsymbol{I}}^{j}(\tilde{\boldsymbol{q}}^{j^*})), \tag{B.1}$$

where $\tilde{I}^{j}(\tilde{q}^{j^*}) = \{l_{ik}^{mn}(\tilde{q}^{j^*}) | \forall i = 1, \dots, N_x, k = 1, \dots, N_y, n = 1, \dots, N_t^j, m = 1, \dots, M\}$, $P_{\tilde{\Lambda}}(x)$ is the unique projection of $x \in \tilde{\Lambda}$ and is defined as $P_{\tilde{\Lambda}}(x) = Argmin\{||y - x||: y \in \tilde{\Lambda}\}$

Proof: As the grid size of the proposed discretization (Δx , Δy and Δt) is positive, the discretized VI problem (Equation 35) could be represented in vector form of $\tilde{I}^j \left(\tilde{q}^{j^*} \right)^T \left(\tilde{q}^j - \tilde{q}^{j^*} \right) \ge 0$ for all $\tilde{q} \in \tilde{\Lambda}$. According to the definition of $P_{\tilde{\Lambda}}$, it could be shown that (Equation (B.2)):

$$|y - P_{\tilde{\Lambda}}(y)| \le |y - z| \tag{B.2}$$

with $P_{\tilde{\Lambda}} \in \tilde{\Lambda}$ and $\tilde{\Lambda}$ is a closed convex set. Let $z = \theta x + (1 - \theta)P_{\tilde{\Lambda}}(y) = P_{\hat{\Lambda}}(y) + \theta(x - P_{\tilde{\Lambda}}(y))$ for all $x \in \tilde{\Lambda}$ and $\theta \in (0, 1)$, Equation (B.2) becomes:

$$\begin{aligned} \left| \boldsymbol{y} - P_{\hat{\Lambda}}(\boldsymbol{y}) \right| &\leq \left| \boldsymbol{y} - P_{\hat{\Lambda}}(\boldsymbol{y}) - \theta \left(\boldsymbol{x} - P_{\hat{\Lambda}}(\boldsymbol{y}) \right) \right| \\ \left| \boldsymbol{y} - P_{\hat{\Lambda}}(\boldsymbol{y}) \right|^{2} &\leq \left| \boldsymbol{y} - P_{\hat{\Lambda}}(\boldsymbol{y}) - \theta \left(\boldsymbol{x} - P_{\hat{\Lambda}}(\boldsymbol{y}) \right) \right|^{2} \\ \left| \boldsymbol{y} - P_{\hat{\Lambda}}(\boldsymbol{y}) \right|^{2} &\leq \left| \boldsymbol{y} - P_{\hat{\Lambda}}(\boldsymbol{y}) \right|^{2} - 2\theta \left(\boldsymbol{y} - P_{\hat{\Lambda}}(\boldsymbol{y}) \right)^{T} \left(\boldsymbol{x} - P_{\hat{\Lambda}}(\boldsymbol{y}) \right) + \theta^{2} \left| \left(\boldsymbol{x} - P_{\hat{\Lambda}}(\boldsymbol{y}) \right) \right|^{2} \\ \left(\boldsymbol{y} - P_{\hat{\Lambda}}(\boldsymbol{y}) \right)^{T} \left(\boldsymbol{x} - P_{\hat{\Lambda}}(\boldsymbol{y}) \right) &\leq \frac{\theta}{2} \left| \left(\boldsymbol{x} - P_{\hat{\Lambda}}(\boldsymbol{y}) \right) \right|^{2} \end{aligned}$$

Thus as $\theta \to 0^+$ it could be shown that (Equation (B.3)):

$$(\boldsymbol{y} - P_{\tilde{\Lambda}}(\boldsymbol{y}))^{T} (\boldsymbol{x} - P_{\tilde{\Lambda}}(\boldsymbol{y})) \le 0$$
(B.3)

(Necessity.) Let $x = \tilde{q}^{j^*}$, which is a solution of the discretized VI problem, and $y = \tilde{q}^{j^*} - \lambda \tilde{I}^j (\tilde{q}^{j^*})$, by Equation (B.3), it could be shown that (Equation (B.4)):

$$\left(\tilde{\boldsymbol{q}}^{j^*} - \lambda \tilde{\boldsymbol{I}}^{j} \left(\tilde{\boldsymbol{q}}^{j^*}\right) - P_{\Lambda} \left(\tilde{\boldsymbol{q}}^{j^*} - \lambda \tilde{\boldsymbol{I}}^{j} \left(\tilde{\boldsymbol{q}}^{*}\right)\right)\right)^{T} \left(\tilde{\boldsymbol{q}}^{*} - P_{\hat{\Lambda}} \left(\tilde{\boldsymbol{q}}^{j^*} - \lambda \tilde{\boldsymbol{I}}^{j} \left(\tilde{\boldsymbol{q}}^{j^*}\right)\right)\right) \leq 0$$
(B.4)

after rearranging will get (Equation (B.5)):

$$\left|\tilde{\boldsymbol{q}}^{j*} - P_{\hat{\Lambda}}\left(\tilde{\boldsymbol{q}}^{j^*} - \lambda \tilde{\boldsymbol{I}}^{j}\left(\tilde{\boldsymbol{q}}^{j^*}\right)\right)\right|^{2} \leq \lambda \tilde{\boldsymbol{I}}^{j}\left(\tilde{\boldsymbol{q}}^{j^*}\right)\left(\tilde{\boldsymbol{q}}^{j^*} - P_{\tilde{\Lambda}}\left(\tilde{\boldsymbol{q}}^{j^*} - \lambda \tilde{\boldsymbol{I}}^{j}\left(\tilde{\boldsymbol{q}}^{*}\right)\right)\right) \tag{B.5}$$

As $P_{\tilde{\Lambda}}(\tilde{q}^{j*} - \lambda \tilde{I}^{j}(\tilde{q}^{j*})) \in \tilde{\Lambda}$ and \tilde{q}^{j*} is the solution of the discretized VI problem, the following equation will hold (Equation (B.6)):

$$\left(P_{\tilde{\Lambda}}\left(\tilde{\boldsymbol{q}}^{j*} - \lambda \tilde{\boldsymbol{I}}^{j}\left(\tilde{\boldsymbol{q}}^{j*}\right)\right) - \tilde{\boldsymbol{q}}^{j*}\right)^{T} \tilde{\boldsymbol{I}}^{j}\left(\tilde{\boldsymbol{q}}^{j*}\right) \ge 0$$
(B.6)

As Equations (B.5) and (B.6) must be simultaneously satisfied, it could be concluded that (Equation (B.7)):

$$\left(P_{\tilde{\Lambda}}\left(\tilde{\boldsymbol{q}}^{j*} - \lambda \tilde{\boldsymbol{I}}^{j}\left(\tilde{\boldsymbol{q}}^{j*}\right)\right) - \tilde{\boldsymbol{q}}^{j*}\right)^{T} \tilde{\boldsymbol{I}}^{j}\left(\tilde{\boldsymbol{q}}^{j*}\right) = 0$$
(B.7)

Owing to the arbitrariness of λ , $P_{\tilde{\Lambda}}\left(\tilde{\boldsymbol{q}}^{j*}-\lambda\tilde{\boldsymbol{I}}^{j}\left(\tilde{\boldsymbol{q}}^{j^*}\right)\right)-\tilde{\boldsymbol{q}}^{j^*}=0$ or $\tilde{\boldsymbol{I}}^{j}\left(\tilde{\boldsymbol{q}}^{j^*}\right)=0$. For $\tilde{\boldsymbol{I}}^{j}\left(\tilde{\boldsymbol{q}}^{j^*}\right)=0$ and by Equation (B.5), it could be shown that $\boldsymbol{q}^{j^*}=P_{\tilde{\Lambda}}\left(\tilde{\boldsymbol{q}}^{j*}\right)$. Thus, in either case it could be concluded that Equation (B.1) is satisfied.

(Sufficiency.) By Equation (B.3), let $y = \tilde{q}^{j^*} - \lambda \tilde{I}^j (\tilde{q}^{j^*})$ and $x = \tilde{q}^j \in \tilde{\Lambda}$, it could be shown that (Equation (B.8)):

$$\left(\tilde{\boldsymbol{q}}^{j^*} - \lambda \tilde{\boldsymbol{I}}^{j} \left(\tilde{\boldsymbol{q}}^{j^*}\right) - P_{\hat{\Lambda}} \left(\tilde{\boldsymbol{q}}^{j^*} - \lambda \tilde{\boldsymbol{I}}^{j^*} (\tilde{\boldsymbol{q}}^{j^*})\right)\right)^T \left(\tilde{\boldsymbol{q}}^{j} - P_{\Lambda} \left(\tilde{\boldsymbol{q}}^{j^*} - \lambda \tilde{\boldsymbol{I}}^{j} (\tilde{\boldsymbol{q}}^{*})\right)\right) \leq 0 \tag{B.8}$$

By Equation (B.1), Equation (B.8) equals (Equation (B.9)):

$$-\lambda \tilde{\boldsymbol{I}}^{j} \left(\tilde{\boldsymbol{q}}^{j^{*}} \right)^{T} \left(\tilde{\boldsymbol{q}}^{j} - \tilde{\boldsymbol{q}}^{j^{*}} \right) \leq 0$$
 (B.9)

As $\lambda \ge 0$, it could be shown that (Equation (B.10)):

$$\tilde{\boldsymbol{I}}^{j} \left(\tilde{\boldsymbol{q}}^{j^*} \right)^{T} \left(\tilde{\boldsymbol{q}}^{j} - \tilde{\boldsymbol{q}}^{j^*} \right) \ge 0 \tag{B.10}$$

which is the vector from the discretized VI problem.

References

Alonso, W. (1964) Location and Land Use. Cambridge: Harvard University Press

Ahn, K., Trani, A.A., Rakha, H. & van Aerde, M. (1999). Microscopic fuel consumption and emission models. Transportation Research Board 78th Annual Meeting, Washington DC.

Ben-Akiva, M., and Bowman, J. L. (1998). Integration of an activity-based model system and a residential location model. Urban Studies, 35(7), 1131-1153.

Bednar-Friedl, B., Koland, O. and Steininger, K.N. (2011) Urban sprawl and policy responses: A general equilibrium analysis of residential choice. Journal of Environmental Planning and Management, 54(1), 145-168

- Bhat, C. R., and Guo, J. (2004). A mixed spatially correlated logit model: Formulation and application to residential choice modeling. Transportation Research Part B: Methodological, 38(2), 147-168.
- Blumenfeld, D.E. (1977) Modeling the joint distribution of home and workplace location in a city. Transportation Science, 11(4), 307-377.
- Boyce, D and Mattsson, L.-G. (1999) Modeling residential location choice in relation to housing location and road tolls on congested urban highway networks. Transportation Research Part B, 33(8), 581-591.
- California Air Resources Board (CARB), (2006). "EMFAC Modeling Change Technical Memo: Redistribution of Heavy-Heavy Duty Diesel Truck Vehicle Miles Traveled in California." www.arb.ca.gov/msei/onroad/techmemo/on-2006-05.pdf.
- Chang, J. S. and Mackett, R. L. (2006). A bi-level model of the relationship between transport and residential location. Transportation Research Part B: Methodological, 40(2), 123-146.
- Dey, P. P., Chandra, S., & Gangopadhaya, S. (2006). Speed distribution curves under mixed traffic conditions. Journal of transportation engineering, 132(6), 475-481.
- Diamond, D.B. (1980) Income and residential location: Muth revisited. Urban Studies, 17(1), 1-12.
- Du, J., Wong, S. C., Shu, C. W., Xiong, T., Zhang, M. P., & Choi, K. (2013). Revisiting Jiang's dynamic continuum model for urban cities. Transportation Research Part B: Methodological, 56, 96-119.
- Ellickson, B. (1981). An alternative test of the hedonic theory of housing markets. Journal of Urban Economics, 9(1), 56-79.
- Frank, M., and Wolfe, P. (1956). An algorithm for quadratic programming. Naval Research Logistics Quarterly, 3(1-2), 95-110.

- Giuliano, G. (1989). Research policy and review 27. New directions for understanding transportation and land use. Environment and Planning A, 21(2), 145-159.
- Goldstein, A. A. (1964). Convex programming in Hilbert space. Bulletin of the American Mathematical Society, 70(5), 709-710.
- Gordon, P., Richardson, H.W., Wong, H.L. (1986) The distribution of population and employment in a polycentric city: the case of Los Angeles. Environment and Planning A, 18(2), 161-173.
- Gwinner (1998) On continuum modeling of large dense networks in urban road traffic. In J.D. Griffiths (ed.) Mathematics in Transport Planning and Control: Proceedings of the Third IMA International Conference on Mathematics in Transport Planning and Control, Pergamon Publishing Company, New York, pp. 321-330.
- Haque, M.B., Choudhury, C. and Hess, S. (2019) Modeling residential location choices with implicit availability of alternatives. The Journal of Transport and Land Use, 12(1), 597-618.
- Hawkins, J. and Habib, K.N. (2018) Spatio-temporal hedonic price model to investigate the dynamics of housing prices in contexts of urban form and transportation services in Toronto. Transportation Research Record, 2672(6), 21-30.
- Ho, H. W., and Wong, S. C. (2005). Combined model of housing location and traffic equilibrium problems in a continuous transportation system. The 16th International Symposium on Transportation and Traffic Theory (ISTTT16). Maryland.
- HO, H. W. & WONG, S. C. (2006). Two-dimensional Continuum Modeling Approach to Transportation Problems. Journal of Transportation Systems Engineering and Information Technology, 6, 53-68.
- Ho, H. W., and Wong, S. C. (2007). Housing allocation problem in a continuum transportation system. Transportmetrica, 3(1), 21-39.

- Hoogendoorn, S.P., Bovy, P.H.L., (2004) Pedestrian route-choice and activity scheduling theory and models. Transport. Res. Part B, 38(2), 169–190.
- Huang, H.J., Lam and W.H.K. (2002) Modeling and solving the dynamic user equilibrium route and departure time choice problem in network with queues. Transportation Research Part B, 36(3), 253-273.
- Leong, H. J. (1968). The distribution and trend of free speeds on two lane two way rural highways in New South Wales. In Australian Road Research Board (ARRB) Conference, 4th, 1968, Melbourne (Vol. 4, No. 1).
- Levitin, E. S., and Polyak, B. T. (1966). Constrained minimization methods. USSR Computational mathematics and mathematical physics, 6(5), 1-50.
- Li, T., Sun, H., Wu J. and Ge, Y. (2017) Optimal toll of new highway in the equilibrium framework of heterogeneous households' residential location choice. Transportation Research Part A, 105, 123-137.
- Li, Z.C., Li, Z.K. and Lam, W.H.K. (2014) An integrated design of sustainable land use and transportation system with uncertainty in future population. Transportmetrica A, 10(2), 160-185,
- Lin, Z.-Y., Wong, S.C., Zhang, P. and Choi K. (2018) A predictive continuum dynamic user-optimal model for the simultaneous departure time and route choice problem in a polycentric city. Transportation Science, 52(6),1496-1508.
- Liu, R., Yu, C., Liu, C., Jiang, J., & Xu, J. (2018). Impacts of haze on housing prices: an empirical analysis based on data from Chengdu (China). International Journal of Environmental Research and Public Health, 15(6), 1161.
- Long, J.C., Szeto, W.Y., Gao, Z.Y., Huang, H.J. and Shi, Q. (2016) The nonlinear equation system approach to solving dynamic user optimal simultaneous route and departure time choice problems. Transportation Research Part B, 83,179-206.

- Long, J.C., Szeto, W.Y., Shi, Q., Gao, Z.Y. and Huang, H.J. (2015) A nonlinear equation system approach to the dynamic stochastic user equilibrium simultaneous route and departure time choice problem. Transportmetrica A, 11(5), 388-C419.
- McLean, J. R. (1989). Two-lane highway traffic operations: Theory and practice (Vol. 11). Taylor & Francis.
- Muth, R.F. (1969). Cities and Housing: The Spatial Pattern of Urban Residential Land Use. Chicago and London: The University of Chicago Press.
- Newman, P. G., & Kenworthy, J. R. (1989). Cities and automobile dependence: A Sourcebook. Brookfield: Gower Technical.
- Ng, K.F. and Lo, H.K. (2015) Optimal housing supply in a bid-rent equilibrium framework. Transportation Research Part B, 74, 62-78.
- Orford, S. (2000). Modeling spatial structures in local housing market dynamics: A multilevel perspective. Urban Studies, 37(9), 1643-1671.
- Owawa, H. and Fujita, M. (1980) Equilibrium land use patterns in nonmonocentric city. Journal of Regional Science, 20(4), 455-475.
- Pasquill, F. (1961). The estimation of dispersion of windborne material. Meteorological Magazine, 90, 22–49.
- Pinjari, A.R., Pendyala, R.M. Bhat, C.R. and Waddell, P.A. (2011) Modeling the choice continuum: an integrated model of residential location, auto ownership, bicycle ownership, and commute tour mode choice decisions. Transportation, 38(6), 933 "C958.
- Rakha, H., AHN, K. and TRANI, A. (2004) Development of VT-micro model for estimating hot stabilized light duty vehicle and truck emissions. Transportation Research Part D, 9, 49-74.

- Rosen, S. (1974). Hedonic prices and implicit markets: Product differentiation in pure competition. Journal of Political Economy, 82(1), 34-55.
- Sasaki, T., Iida, Y and Yang, H. (1990) User-equilibrium traffic assignment by continuum approximation of network flow. Proceedings of 11th International Symposium on Transportation and Traffic Theory, Yokohama, Japan, July 1990, pp. 233-252.
- Schirmer, P.M., van Eggermond, M.A.B. and Axhausen, K.W. (2014) The role of location in residential location choice models: a review of literature. The Journal of Transport and Land Use, 7(2), 3-21.
- Scora, G. and Barth, M. (2006) Comprehensive Modal Emissions Model (CMEM), version 3.01: User's Guide. University of California, Riverside Center for Environmental Research and Technology.
- Sener, I.N., Pendyala, R.M. and Bhat, C.R. (2011) Accommodating spatial correlation across choice alternatives in discrete choice models: an application to modeling residential location choice behaviour. Journal of Transport Geography, 19(2), 294-303.
- Stockie, J. M. (2011). The mathematics of atmospheric dispersion modeling. SIAM Review, 53(2), 349–372.
- Sullivan, D. M. (2017). The true cost of air pollution: Evidence from the housing market. Working paper, Resources for the Future, Washington, DC.
- Taguchi, A and Iri, M. (1982) Continuum approximation to dense networks and its application to the analysis of urban road networks. Mathematical Programming Study, 20, 178-217.
- Tornberg A.K. and Engquist B. (2004) Numerical approximations of singular source terms in differential equations. Journal of Computational Physics, 200(2): 462-488.

- United States Environmental Protection Agency EPA (1994) User's Guide to MOBILE 5 (Mobile Source Emission Factor Model), Environmental Protection Agency, Ann Arbor, Michigan. Vaughan, R. (1987). Urban Spatial Traffic Patterns, London, Pion.
- Vaughan, R. (1987). Urban Spatial Traffic Patterns, London, Pion.
- Viti, F., Hoogendoorn, S. P., van Zuylen, H. J., Wilmink, I. R., & van Arem, B. (2008, October). Speed and acceleration distributions at a traffic signal analyzed from microscopic real and simulated data. In 2008 11th international IEEE conference on intelligent transportation systems (pp. 651-656). IEEE.
- Wagner, P., and Wegener, M. (2007). Urban land use, transport, and environment models. Experiences with an integrated microscopic approach. DisP-The Planning Review, 43(170), 45-56.
- Wardman, M. and Bristow, A.L. (2004). Traffic related noise and air quality valuations: Evidence from stated preference residential choice models. Transportation Research Part D: Transport and Environment, 9(1), 1-27.
- Whaley, H. (1974). The derivation of plume dispersion parameters from measured three-dimension data. Atmospheric Environment,8(3), 281–290.
- Wheaton, W. C. (1977). Income and urban residence: An analysis of consumer demand for location. American Economic Review, 67(4), 620-631.
- Yang, L., Li, T., Wong, S.C., Shu, C.W. and Zhang, M. (2018) Modeling and simulation of urban air pollution from the dispersion of vehicle exhaust: A continuum modeling approach. International Journal of Sustainable Transportation, 13(10), 722-740
- Yim, K.K.W., Wong S.C., Chen, A., Wong, C.K. and Lam W.H.K. (2011) A reliability-based land use and transportation optimization model. Transportation Research Part C, 19(2), 351-362.

- Yin, J., Wong, S. C., Sze, N. N. and Ho, H.W. (2013). A continuum model for housing allocation and transportation emission problems in a polycentric city. International Journal of Sustainable Transportation, 7(4), 275-298.
- Yin, J., Wong, S.C., Choi, K. and Du, Y.C. (2017). Continuum modeling approach to the spatial analysis of air quality and housing location choice. International Journal of Sustainable Transportation, 11(5), 319-329.
- Ying, J.Q. (2015) Optimization for multiclass residential location models with congestible transportation networks. Transportation Science, 49(3), 452-471.
- Zolfaghari, A., Sivakumar, A. and Polak, J.W. (2012) Choice set pruning in residential location choice modeling: A comparison of sampling and choice set generation approaches in Greater London. Transportation Planning and Technology, 35(1), 87-106.